Physics – Uspekhi **39** (1) 31 – 56 (1996) ©1996 Uspekhi Fizicheskikh Nauk, Russian Academy of Sciences

REVIEWS OF TOPICAL PROBLEMS PACS number: 61.50K, 61.70B, 64.80, 70.00

Atomic and vacancy ordering in nonstoichiometric carbides

A A Rempel'

Contents

Abstract. An analysis of the electronic structure of highly nonstoichiometric transition-metal carbides in both ordered and disordered states is given, which explains the influence of atomic and vacancy order on the physical properties of the carbides. It is shown that the dependence of carbide properties on the arrangement of carbon atoms in the nonmetal sublattice is related to both the symmetry space group of the crystal and the symmetry of the nearest-neighbour environment of the carbide atoms. By analysing order–disorder phase transition data, experimental information on atomic and vacancy order in carbides is obtained in order to explain the nature of superstructures at high vacancy concentrations.

1. Introduction

Carbides of the group-IV and group-V transition metals occupy a special place among nonstoichiometric compounds. They have a simple — and similar — structure and possess extended homogeneity regions. Along with nitrides and lower cubic oxides, they group into what is often referred to as substitutional phases (compounds, alloys), variable composition compounds [1 – 7], or, most aptly, nonstoichiometric substitutional compounds [8].

The atomic ordering of the nonstoichiometric compounds is a widespread but, compared to metal alloys, little studied phenomenon — especially as far as its influence on the electronic structure and material properties is concerned. This is presumably due to the difficulties one faces in disentangling ordering and composition effects, something which requires particularly careful and highly accurate experimentation.

A A Rempel Institute of Solid State Chemistry, Ural Division of the Russian Academy of Sciences, Pervomaiskaya 91, Ekaterinburg, 620219, Russia
Fax (7-3432) 44-44 95
E-mail: rempel@gusev.e-burg.su.

Received 20 March 1995, revised 5 July 1995
Uspekhi Fizicheskikh Nauk **166** (1) 33–62 (1996)
Translated by E Strel'chenko, edited by S D Danilov

The reason for atomic ordering in nonstoichiometric carbides is the perturbation of the atomic and electronic structure due to vacancies introduced into the nonmetal lattice. Although the metal sublattice does not change its symmetry to a first approximation, it does suffer distortion: there are static displacements locally of the atoms relative to the vacancies and there is also a change in the average atomic spacing (i. e., the lattice parameter). As for the nonmetal atoms, they rearrange themselves in their sublattice in addition to undergoing local static displacements. Naturally, these structural changes should have a significant effect on the physical and chemical properties of the nonstoichiometric carbides, and it is this effect which is the subject of the present review.

2. Crystal structure

2.1 Carbides as nonstoichiometric interstitial compounds

The term 'nonstoichiometric' generally covers all compounds in which a high concentration of atomic defects exists even in the absence of impurity atoms. However, since perfect defect-free crystals do not exist at all, in itself the presence of defects does not imply nonstoichiometry. The essential feature of nonstoichiometry is a thermodynamically equilibrium defect (vacancy) concentration which secures interaction between the defects. The term nonstoichiometric should therefore be referred to compounds with homogeneity regions having at least minimal vacancy concentrations capable of securing the vacancy–vacancy interaction. Among these are cubic MC_y ($MC_y\square_{1-y}$) and hexagonal M_2C_y ($M_2C_y\,\square_{1-y}$) carbides of the group-IV and -V transition metals ($\square$ denoting a structural vacancy).

A structural feature of MC_y and M_2C_y carbides is that carbon atoms occupy (either all or some of) the octahedral interstitials of the metal sublattice. The carbon atoms and unoccupied interstitials of the metal sublattice (structural vacancies) form in the nonmetal sublattice a substitutional alloy in which a structural vacancy is the analogue of a nonmetal interstitial atom. The concentration of the structural vacancies in the nonmetal sublattice determines the

nonstoichiometry of the carbide (i. e., the deviation from the stoichiometric $MC_{1.00}$ or $M_2C_{1.00}$) and may be as high as 30 to 60 at. percent at the lower homogeneity bound. This is indicative of the extremely high stability of carbide lattices to the formation of structural vacancies. In contrast to all other compounds — and along with the cubic nitrides MN_y — the MC_y carbides may, their structure unaltered, vary all the way from $MC_{1.00}$ to $MC_{0.35-0.40}$ in chemical composition.

The group-IV transition metals (Ti, Zr, Hf) have the hexagonal close-packed (hcp) structure and form MC_y carbides only with a face-centred (fcc) metal sublattice. The transition body-centred (bcc) structure metals (V, Nb, Ta) form MC_y's with an fcc metal sublattice or M_2C_y's with the hcp metal sublattice.

The high concentration of structural vacancies in a crystal is one of the most important properties of the nonstoichiometric interstitial compounds. The presence of defects has a very important influence on compound properties. This is the reason why most studies of the 70–80s were concerned with how compound properties depend on the relative content of metal, nonmetal, and vacancies. On the other hand, when discussing the structure and properties of the nonstoichiometric interstitial compounds, it has been shown in recent years that not only the relative number of atoms and vacancies, but also the nature of their arrangement in the lattice should be considered.

In nonstoichiometric MC_y and M_2C_y carbides with vacancies ($y < 1.0$) the number of lattice positions exceeds that of the atoms in them. Under certain conditions, carbon atoms are distributed in a random and disordered manner over the available positions, and disordered nonstoichiometric carbides do not therefore possess the translational symmetry characteristic of a stoichiometric crystal. However, the random distribution of carbon over nonmetal sublattice sites implies equal site-occupation probabilities, and hence all the nonmetal sites are equivalent crystallographically. In other words, the disordered nonstoichiometric carbides have a translational symmetry of a certain 'site-occupation probability lattice'.

For vacancy-rich nonstoichiometric carbides, a disordered state is thermodynamically equilibrium above the order–disorder phase transition temperature T_{trans} which varies from 900 to 1500 K depending on the carbide type. For $T < T_{\text{trans}}$, only the ordered state of these compounds is thermodynamically equilibrium, but to attain it generally requires long annealing or another special kind of thermal treatment. In contrast, the disordered state easily survives an ordinary cooling or quenching of a high-temperature- sintered carbide, and is stable enough to exist as metastable at $T < T_{\text{trans}}$. Note that at fixed temperature a nonstoichiometric carbide of a given composition has different properties in its ordered and metastable disordered states [9].

The ease of preparation of a disordered state by direct synthesis of nonstoichiometric carbides has led to a widespread misconception that the disordered arrangement of atoms and vacancies is the main if not the only structural state possible for these compounds. For this reason, in most experimental studies in the 60s and 70s the structural state of the nonstoichiometric interstitial compounds — including the group-IV and -V transitions metal carbides — was considered to be irrelevant. The property differences at the same composition were usually explained in terms of experimental errors and composition uncertainties. Only advances in experimental techniques, and particularly neutron-diffraction structure studies revealed that, under certain conditions, nonmetal interstitials and structural vacancies may be arranged in an ordered manner in nonstoichiometric interstitial compounds.

Group-IV metals (Ti, Zr, Hf) form only TiC_y, ZrC_y and HfC_y monocarbides with the $B1$(NaCl)-type structure, whose compositions may deviate considerably from the stoichiometric $MC_{1.00}$ ($0.35 \leqslant y \leqslant 1.00$).

Group-V metals Va, Nb, and Ta, along with the cubic $VC_{y'}$, NbC_y and TaC_y carbides, form disordered lower carbides V_2C, Nb_2C and Ta_2C with the hcp $L'3$ (W_2C)-type structure at high temperatures. The homogeneity regions of the monocarbides MC_y of the group-V metals, while narrower than for the group-IV monocarbides, are still wide enough ($0.70 \leqslant y \leqslant 1.00$). In contrast to other group-IV and -V transition metal carbides, for the cubic VC_y the upper homogeneity boundary is, under normal conditions, the nonstoichiometric carbide $VC_{0.87}$ containing a high concentration of structural vacancies in its carbon sublattice.

Thus, the nonstoichiometric carbides we are considering crystallise in the face-centred cubic and hexagonal close-packed structures. These can be thought of as a sequence of alternating atomic layers. For $B1$(NaCl)-structure monocarbides, planes with either only metal or only nonmetal atoms alternate in the direction perpendicular to $[111]_{B1}$ (or equivalently to $[1\bar{1}1]_{B1}$, $[\bar{1}11]_{B1}$ and $[\bar{1}\bar{1}1]_{B1}$. The metal- atom planes, as far as their relative position is concerned, give the sequence $ABC\ ABC\ldots$, the closest cubic-law packing. Denoting by X, Y, and Z the layers formed by the (both occupied and vacant) nonmetal sublattice sites (the Y and Z layers are shifted relative to X in the same way as B and C relative to A), the general sequence of the atomic layers will be $AXBYCZ\ AXBYCZ\ldots$.

2.2 Ordered carbides

Atomic ordering viewed as the disorder–order structural phase transition results from the atoms being rearranged over the lattice sites of the substitution solid solution. In a disordered state the interchangeable solution components are distributed randomly over the sites of a certain crystal lattice, and the probability for any site to be occupied by an atom of a given type is just the concentration of such atoms. As the temperature is lowered, a disorder–order phase transition occurs, with the result that the lattice sites of the disordered solution group into a number of sublattices. The sublattices of an ordered solution differ in the probability of finding a given type of atom in their sites.

The phenomenon of ordering is not limited to substitution solutions. It may also occur in interstitial solutions if there is more interstitial positions than atoms to be accommodated. As an interstitial solution is getting ordered, the empty positions and the interstitial atoms appear as a substitution solution between them, whereas the solvent atoms form a stationary atomic framework, with interstitial atoms and vacancies rearranged within it.

Thus, the presence of structural vacancies in nonstoichiometric carbides may lead to ordering under certain conditions. In disordered nonstoichiometric carbides, carbon atoms are distributed statistically over the sites of the defective (i. e., containing structural vacancies) nonmetal sublattice. As a result of cooling-induced ordering, the disordered nonmetal sublattice divides itself, in the simplest case, into two sublattices, one made up of carbon atoms, and the other, of structural vacancies. The ordering reduces the

symmetry of the space group of the crystal, since some of the symmetry transformations of the disordered nonmetal lattice — those bringing the occupied into unoccupied sites — will not be among the symmetry elements of the ordered crystal because these sites become crystallographically nonequivalent.

A detailed description of various superstructures occurring in nonstoichiometric carbides may be found in Refs [8, 10 – 12]. We can therefore restrict our attention to the summary of the most typical ordered phases (Table 1).

From neutron diffraction data [13, 14], the nonstoichiometric carbides of titanium and zirconium form ordered cubic M_2C-type phases upon a slow cooling from 1200 – 1400 K; the lattice parameter of these superstructures being twice that of the disordered carbides. The kinetics of formation of the cubic Ti_2C superstructure [50] shows this ordering to be a first-order transition. The M_2C-type ordered phases of the carbides of titanium and zirconium are believed to be of trigonal symmetry [15, 18].

According to theoretical calculations [17, 20 – 23], the TiC_y and ZrC_y carbides may form M_2C, M_3C_2, and M_6C_5 ordered phases depending on the carbon content, and in the nonstoichiometric hafnium carbide HfC_y the Hf_3C_2 and Hf_6C_5 phases may appear.

In the vanadium carbide VC_y, the trigonal (space group $P3_1$) and monoclinic (space group $C2$) ordered V_6C_5 phases have been found [27 – 29]. Monoclinic ordered V_6C_5 (space group $C2/m$) was observed in an electron microscope study of long-range order (lro) in vanadium carbide [51]. It has also been found that at 1460 K vanadium carbide exhibits a disorder–order transition that leads to the formation of the ordered cubic V_8C_7 phase [31 – 33]. Note that the superstructure M_8X_7 has not been seen in any other nonstoichiometric interstitial compounds, and judging from calculations [8, 21, 23, 52], its formation is not possible for MX_y compounds with a homogeneity region with $y \approx 1.00$ as the upper boundary. In VC_y the V_8C_7 superstructure appears to be a boundary effect, due to the fact that the upper boundary of the homogeneity region of disordered VC_y is at $y = 0.87$ and not at $y = 1.00$ as in other nonstoichiometric compounds.

For the nonstoichiometric niobium monocarbide NbC_y, electron microdiffraction [28, 35] and neutron diffraction [36 – 42] ordering studies have shown that on annealing under 1300 K, the $NbC_{0.83}$ ordered phase forms over a wide range of compositions near Nb_6C_5. It is believed [28, 35, 36] that the ordered Nb_6C_5 has the trigonal structure analogous to that of V_6C_5 [27]. It is argued [38 – 42, 51, 53] that the Nb_2C_5 superstructure is monoclinic and that the unit cell of this ordered phase belongs to the space group $C2/m$.

It is shown [21 – 24] that near the lower homogeneity boundary of NbC_y at $T < 900$ K, the $NbC_{0.67}$ – $NbC_{0.71}$ ordered phase with a rhombic or monoclinic lattice can exist in the narrow range Nb_3C_2.

An electron diffraction study on $TaC_{0.83}$ [54] revealed a diffusion band with geometry corresponding to the highly

Table 1. Ordered phases of nonstoichiometric carbides in M – C systems (M: Ti, Zr, Hf, V, Nb, Ta)

Ordered phase			Basic phase			References
composition formula	range of existence of the phase, or carbon content (at. %)	lattice type (symmetry)	space group	composition formula	lattice type	
1	2	3	4	5	6	7
Ti_2C	$TiC_{0.52}$ – $TiC_{0.71}$	cubic	$Fd3m$	TiC	$B1$	[13, 14]
Ti_2C	33.0 – 43.0	trigonal	$P3_121$	TiC	$B1$	[15]
Ti_3C_2	$TiC_{0.64}$ – $TiC_{0.68}$	rhombic	$C222_1$	TiC	$B1$	[16]
Ti_2C	$TiC_{0.47}$ – $TiC_{0.54}$			TiC	$B1$	[17]
Ti_3C_2	$TiC_{0.62}$ – $TiC_{0.70}$			TiC	$B1$	[17]
Ti_6C_5	$TiC_{0.80}$ – $TiC_{0.90}$			TiC	$B1$	[17]
δ' – ZrC_x	39.0 – 43.0	trigonal		ZrC	$B1$	[18]
ZrC_x	$ZrC_{0.63}$ – $ZrC_{0.74}$	cubic		ZrC	$B1$	[14]
$ZrC_{0.75}$	$ZrC_{0.69}$ – $ZrC_{0.77}$	cubic		ZrC	$B1$	[19]
Zr_2C	$ZrC_{0.47}$ – $ZrC_{0.54}$			ZrC	$B1$	[8, 20–24]
Zr_3C_2	$ZrC_{0.60}$ – $ZrC_{0.71}$			ZrC	$B1$	[8, 20–24]
Zr_6C_5	$ZrC_{0.76}$ – $ZrC_{0.92}$			ZrC	$B1$	[8, 20–24]
Hf_3C_2	$HfC_{0.67}$ – $HfC_{0.72}$			HfC	$B1$	[8, 20–25]
Hf_6C_5	$HfC_{0.77}$ – $HfC_{0.90}$			HfC	$B1$	[8, 20–25]
β_p–V_2C	33.0 ($VC_{0.5}$)	rhombic, ζ – Fe_2N type	$Pbcn$	V_2C	$L'3$	[18,26]
β'–V_2C	33.0 ($VC_{0.5}$)	hexagonal		V_2C	$L'3$	[18, 26]
V_6C_5	45.5 ($VC_{0.83}$)	trigonal	$P3_1$	VC_y	$B1$	[27]
V_6C_5	45.5 ($VC_{0.83}$)	monoclinic	$C2$	VC_y	$B1$	[28, 29]
δ–VC_x	45.5 ($VC_{0.83}$)	trigonal		VC_y	$B1$	[18]
δ''_M–VC_x	45.0 – 47.0	monoclinic		VC_y	$B1$	[30]
V_8C_7	46.6 ($VC_{0.87}$)	cubic	$P4_332$	VC_y	$B1$	[31–33]
Nb_2C	33.3 ($NbC_{0.5}$)	rhombic, ζ – Fe_2N type	$Pnma$	Nb_2C	$L'3$	[34]
Nb_2C	33.3 ($NbC_{0.5}$)	hexagonal, ε – Fe_2N type		Nb_2C	$L'3$	[34]
Nb_6C_5	$NbC_{0.75}$ – $NbC_{0.84}$	trigonal		NbC	$B1$	[28, 35–37]
Nb_6C_5	$NbC_{0.81}$ – $NbC_{0.88}$	monoclinic	$C2/m$	NbC	$B1$	[38–42]
Nb_3C_2	$NbC_{0.67}$ – $NbC_{0.71}$			NbC	$B1$	[8, 20–24]
Nb_6C_5	$NbC_{0.78}$ – $NbC_{0.90}$			NbC	$B1$	[8, 20–24]
Ta_2C	33.3 ($TaC_{0.5}$)	trigonal		Ta_2C	$L'3$	[43]
Ta_6C_5	$TaC_{0.79}$ – $TaC_{0.89}$	incommensurate phase		TaC	$B1$	[44–49]
Ta_6C_5	$TaC_{0.81}$ – $TaC_{0.89}$			TaC	$B1$	[8, 20–24]

disordered M_6C_5 arrangement. Thermodynamical calculations of the disorder–order phase transition in tantalum carbide and of the equilibrium Ta–C phase diagram [8, 10, 20 – 23, 55, 56] show the M_6C_5 superstructure to be the only ordered phase possible for tantalum carbide.

A neutron diffraction ordering study of TaC_y [47 – 49] showed that an incommensurate superstructure close to $TaC_{0.79}$ – $TaC_{0.89}$ forms in the composition range M_6C_5.

Because of the large number of superstructures that form in them, nonstoichiometric carbides are convenient objects for the study of atom–vacancy ordering. The experimental results summarised in Refs [8, 10, 11, 57] and briefly discussed in this section show that, crystallographically, the nonstoichiometric carbides MC_y with basic $B1$ structure may exhibit ordered phases of the types M_2C (space group $R\bar{3}m$, $Fd3m$, $I4_1/amd$, $P4/mmm$), M_3C_2 ($C222_1$, $Immm$, $P2$, $P\bar{3}m1$), M_4C_3 (Pm3m, 14/mmm), M_6C_5 ($C2/m$, $P3_1$, $C2$), and M_8C_7 ($Fm3m$, $P4_332$), or generally $M_{2t}C_{2t-1}$ ($t = 1; 1, 5; 2; 3; 4$.

Earlier symmetry analysis of all of the superstructures crystallographically permissible in the nonstoichiometric cubic carbides [12, 52] has revealed a structural disorder–order transition channel for each particular superstructure: a set of all nonequivalent, superstructural reciprocal vectors $\mathbf{k}_s^{(j)}$ located within the site-centred first Brillouin zone for the basic disordered lattice ($\mathbf{k}_s^{(j)}$ is the jth arm of the star of the wave vector $\{\mathbf{k}_s\}$; here and hereafter, the wave vector stars for the first Brillouin zone of a fcc crystal are numbered according to Refs [58] and [59], and the arms, according to Ref. [10]).

Symmetry analysis shows [12] that the formation of a superstructure in the carbide may be associated with one or more $\{\mathbf{k}_s\}$ stars. To each $\{\mathbf{k}_s\}$ star there corresponds an lro parameter η_s, i. e., the number of the lro parameters describing a superstructure equals that of the superstructure wave vector stars.

There are both Lifshitz and non-Lifshitz types among the carbide phase transitions stars. To the Lifshitz (symmetrical) stars there correspond points in the Brillouin zone that have a certain set of symmetry elements. The set secures either an identical transformation of the points or their translation into equivalent positions. Such a set necessarily includes axes intersecting one another or symmetry planes, or it possesses inversion. Thus, the wave vector group of a Lifshitz point in the Brillouin zone must have point-intersecting symmetry elements (such groups are said to possess a central point).

While Lifshitz star arms are written in terms of the basic reciprocal lattice vectors by use of fixed numerical parameters (e. g., the first arms of the $\{\mathbf{k}_8\}$, $\{\mathbf{k}_9\}$, $\{\mathbf{k}_{10}\}$ and $\{\mathbf{k}_{11}\}$ stars of the fcc-lattice Brillouin zone), for general non-Lifshitz stars $\mathbf{k}_0^{(1)} = \mu_1\mathbf{b}_1 + \mu_2\mathbf{b}_2 + \mu_3\mathbf{b}_3$ the parameters μ_i for vectors $\mathbf{b}_i$ are not contingent on any symmetry factors.

A necessary condition for a phase transition of the second kind is an identically zero coefficient of the cubic term in the expansion of the free energy in terms of the lro parameter [60, 61]. This is possible if the symmetry cube of the irreducible representation responsible for the transition does not contain a unitary representation of the disordered crystal's space symmetry group. If a change in translation symmetry is involved, then the group-theoretical Landau criterion is equivalent to the following necessary condition [62]: a second-order transition is possible only if among the phase transition star vectors no three (not necessarily different) vectors can be chosen whose sum either vanishes or equals a structural vector $\mathbf{H}$ of the disordered crystal's reciprocal lattice. Thus, for a second-order phase transition

$$\left.\begin{array}{r}\mathbf{k}_s^{(j_1)} + \mathbf{k}_s^{(j_2)} + \mathbf{k}_s^{(j_3)} \\ 3\mathbf{k}_s^{(j)}\end{array}\right\} \neq 0 \quad \text{or} \quad \neq \mathbf{H}\,. \tag{1}$$

The condition (1) applies if the space group of the ordered phase is a symmetry subgroup of the disordered one, which is true for all the carbide superstructures under discussion.

The disorder–order transitions MC_y – M_2C (space groups $R\bar{3}m$, $Fd3m$, $I4_1/amd$) are associated with either the $\{\mathbf{k}_9\}$ or $\{\mathbf{k}_8\}$ Lifshitz stars, for which (i) the condition (1) is always met, and (ii) these transitions satisfy the Landau criterion for second-order phase transitions.

The phase transition channels involving the formation of tetragonal superstructures M_2C (space group $P4/mmm$) and M_4C_3 (space group $I4/mmm$) and of cubic superstructures M_4C_3 (space group $Pm3m$) and M_8X_7 (space group $Fm3m$) include either the arms of the $\{\mathbf{k}_{10}\}$ star alone, or also the arms of $\{\mathbf{k}_9\}$ and $\{\mathbf{k}_8\}$. For the $\{\mathbf{k}_{10}\}$ star the condition (1) is not fulfilled, so the formation of these superstructures can only be a first-order phase transition.

The formation of the M_3C_2 superstructure involves a distortion of symmetry for one or two of the non-Lifshitz $\{\mathbf{k}_5\}$, $\{\mathbf{k}_4\}$, or $\{\mathbf{k}_3\}$ stars; also, the transition channel for each of these superstructures contains a superstructure vector $\mathbf{k}_s^{(j)}$ which when tripled coincides with one of the reciprocal lattice sites: for rhombic (space groups $Immm$ and $C222_1$) superstructures $3\mathbf{k}_4^{(1)} = (220)$, for the monoclinic ($P2$) and trigonal ($P3m1$) superstructures $3\mathbf{k}_4^{(5)} = (202)$ and $3\mathbf{k}_5^{(6)} = (1\bar{1}1)$, respectively. This means that condition (1) is not obeyed and that the formation of disordered M_3C_2 phases is a first-order phase transition.

For the cubic superstructure M_8C_7 (space group $P4_332$), the phase transition channel includes all arms of the Lifshitz stars $\{\mathbf{k}_9\}$ and $\{\mathbf{k}_8\}$, and those of the non-Lifshitz star $\{\mathbf{k}_4\}$; the sum $(\mathbf{k}_4^{(1)} + \mathbf{k}_4^{(5)} + \mathbf{k}_4^{(9)})$ of all the three superstructure channel vectors being equal to the reciprocal lattice vector (111). Clearly the formation of this superstructure can only be a first-order transition.

The generic superstructure type for all nonstoichiometric carbides MC_y with basic structure $B1$ (NaCl) is M_6C_5. The determination of phase transition channels [10, 12, 63, 64] showed that the formation of the M_6C_5 superstructure is associated with several wave vector stars (Table 2), each with a corresponding lro parameter. To estimate the type of the phase transition, only the critical order parameters for non-Lifshitz stars must be considered. For the monoclinic (space group $C2/m$) and trigonal ($P3_1$) M_6C_5 superstructures, the critical order parameters correspond to the $\{\mathbf{k}_4\}$ and $\{\mathbf{k}_3\}$ stars. For the $C2$ monoclinic M_6C_5 superstructure, critical order parameters correspond to $\{\mathbf{k}_4\}$, $\{\mathbf{k}_3\}$, and $\{\mathbf{k}_0\}$. Thus, for all three M_6C_5 superstructures the number of critical parameters is more than one. The simultaneous distortion of symmetry in several irreducible representations implies that the disorder–order transitions MC_y – M_6C_5 are first-order transitions.

For the experimentally observed M_6C_5 and M_8C_7 ($P4_332$) superstructures, the conclusion about the first-order phase transitions is supported by the results of Refs [36, 38, 40, 42, 44 – 47, 65 – 68].

Analysis suggests that only M_2C superstructures (space groups $R\bar{3}m$, $Fd3m$, and $I4_1/amd$) can form by a second-order mechanism. The formation of the superstructures M_2C

Table 2. $MC_y - M_6C_5$ disorder–order transition channels in nonstoichiometric $B1$ carbides MC_y [12, 63]

Ordered phase symmetry	Space group	Nonequivalent superstructure vectors forming the disorder–order transition channel
monoclinic	$C2/m$	$\mathbf{k}_9^{(3)} = \mathbf{b}_2/2$,
		$\mathbf{k}_4^{(1)} = (\mathbf{b}_1 + \mathbf{b}_2 + 2\mathbf{b}_3)/3,\ \mathbf{k}_4^{(2)} = -\mathbf{k}_4^{(1)}$,
		$\mathbf{k}_3^{(3)} = -(4\mathbf{b}_1 + \mathbf{b}_2 + 2\mathbf{b}_3)/6,\ \mathbf{k}_3^{(4)} = -\mathbf{k}_3^{(3)}$
triclinic	$P3_1$	$\mathbf{k}_9^{(3)}$,
		$\mathbf{k}_4^{(1)},\ \mathbf{k}_4^{(2)}$,
		$\mathbf{k}_4^{(7)} = (\mathbf{b}_3 - \mathbf{b}_1)/3,\ \mathbf{k}_4^{(8)} = -\mathbf{k}_4^{(7)}$,
		$\mathbf{k}_4^{(9)} = (2\mathbf{b}_1 + \mathbf{b}_2 + \mathbf{b}_3)/3,\ \mathbf{k}_4^{(10)} = -\mathbf{k}_4^{(9)}$,
		$\mathbf{k}_3^{(3)},\ \mathbf{k}_3^{(4)}$,
		$\mathbf{k}_3^{(9)} = (2\mathbf{b}_1 + 3\mathbf{b}_2 + 4\mathbf{b}_3)/6,\ \mathbf{k}_3^{(10)} = -\mathbf{k}_3^{(9)}$,
		$\mathbf{k}_3^{(23)} = (2\mathbf{b}_1 + \mathbf{b}_2 - 2\mathbf{b}_3)/6,\ \mathbf{k}_3^{(24)} = -\mathbf{k}_3^{(23)}$
monoclinic	$C2$	$\mathbf{k}_9^{(3)}$,
		$\mathbf{k}_4^{(1)},\ \mathbf{k}_4^{(2)}$,
		$\mathbf{k}_3^{(3)},\ \mathbf{k}_3^{(4)}$,
		$\mathbf{k}_0^{(4)} = (4\mathbf{b}_1 + \mathbf{b}_2 - 4\mathbf{b}_3)/12,\ \mathbf{k}_0^{(28)} = -\mathbf{k}_0^{(4)}$,
		$\mathbf{k}_0^{(13)} = -(8\mathbf{b}_1 + 5\mathbf{b}_2 + 4\mathbf{b}_3)/12,\ \mathbf{k}_0^{(37)} = -\mathbf{k}_0^{(13)}$

$\mathbf{b}_1 = (\bar{1}11)$, $\mathbf{b}_2 = (1\bar{1}1)$, and $\mathbf{b}_3 = (11\bar{1})$ are the basic vectors of the reciprocal lattice (in units of $2\pi/a_{B1}$)

($P4/mmm$), M_3C_2, M_4C_3, M_6C_5, and M_8C_7 in MC_y $B1$ carbides may only be a first-order phase transition.

Analysis of the short-range order (sro) to long-range order (lro) relationship [69 – 72] in systems under ordering (A_yB_{1-y}, $MX_y\,\square_{1-y}$) indicates an important correlation feature, in that if the system may have a maximum-sro no-lro structure, then the disorder–order transformation occurs as a first-order phase transition; otherwise, when the attainment of the maximum (or lower) sro in the first coordination sphere leads to lro, it is second order. This was confirmed in Refs [69 – 72] in ordering studies on the bcc and fcc solid solutions (alloys) A_yB_{1-y} and nonstoichiometric interstitial $B1$ $MX_y\,\square_{1-y}$ compounds. In particular, it is shown that ordering in bcc alloys may be a second-order phase transition, whereas the formation of the superstructures $M_{2t}X_{2t-1}$ ($t = 1$; 1, 5; 2; 3; 4) of nonstoichiometric MX_y compounds is a first-order phase transition. This is consistent with the earlier conclusions about the kind of disorder–order transitions in the nonstoichiometric carbides.

By and large, the literature abounds with experimental and theoretical studies on the structure of ordered phases of nonstoichiometric carbides. The changes in their properties at disorder–order transitions are much less studied though, as are their properties in various structural states.

2.3 Basic lattice parameter

The effect of nonstoichiometry on the lattice parameter of the basic crystal lattice of nonstoichiometric $B1$ (NaCl)-type carbides has been studied by many authors. It is found that reducing carbon content, or equivalently increasing the concentration of structural vacancies, brings about a linear decrease in the lattice parameter of the compound.

The ordering of a nonstoichiometric MC_y carbide not only reduces the lattice symmetry but also involves a change in the lattice parameter of its basic cubic lattice.

The influence of ordering on the basic lattice parameter was found in a study of the structural disorder–order phase transition in the nonstoichiometric niobium carbide NbC_y [38, 40, 41]. It turned out that within the homogeneity region of the ordered Nb_6C_5 phase the lattice parameter of the ordered niobium carbide exceeds that of disordered carbide NbC_y of the same carbon content. The lattice parameter difference $\Delta a = a(y, \eta) - a(y, 0)$ between the ordered and disordered niobium carbide varied with carbon content.

Later, a lattice parameter increase was observed at the $VC_{0.89} - V_8C_7$ transition in a vanadium carbide ordering study [67]. At room temperature the basic lattice parameter of quenched disordered carbide $VC_{0.89}$ was 4.1662 A, whereas in the ordered carbide of the same composition it was 4.1667 A (i. e., 8.3334 A for the cubic superstructure V_8C_7, whose lattice parameter is twice that for the basic lattice). This compares favourably with high-temperature X-ray results which show a sudden change from 4.202 to 4.200 A in the basic lattice parameter of vanadium carbide at the order-disorder transition at $T = 1410 \pm 20$ K.

Investigations [73] showed that the basic lattice parameter of ordered tantalum carbide is greater than for the quenched disordered TaC_y of the same carbon content.

A detailed study of the basic lattice parameter as a function of the degree of order was carried out on niobium and tantalum carbides in Ref. [74]. The lattice parameter was measured by a standard X-ray photography method at a stabilised temperature of 294 K. The lro due to carbon-vacancy rearrangement was examined by neutron diffraction.

Figure 1 shows the variation with carbon content of the basic lattice parameter in niobium and tantalum carbides in disordered and ordered states.

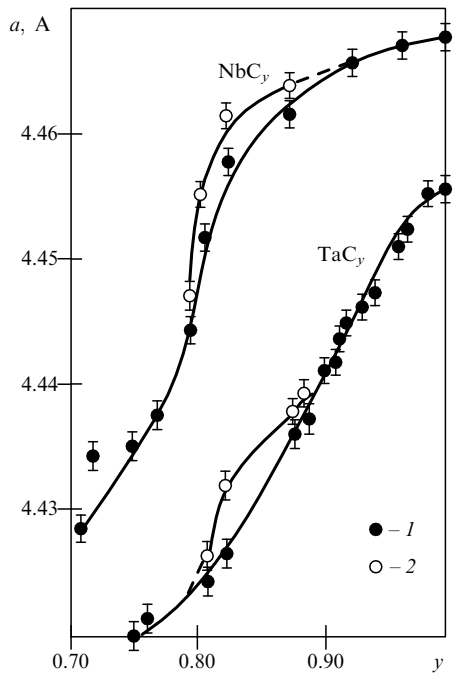

Figure 1. The dependence of the period of the basic *B*1-type crystal lattice on the composition of NbC_y and TaC_y carbides in disordered (*1*) and ordered (*2*) states (after Ref. [74]).

As in the earlier studies [38, 75 – 78], as the vacancy concentration increased, the lattice parameter decreased nonlinearly in monocarbides of Nb and Ta. In the region where the nonstoichiometry of the MC_y carbides is relatively small ($0.9 < y < 1.0$), increasing vacancy concentration has a stronger effect on the lattice parameter of TaC_y as compared to NbC_y (Fig. 1). This indicates that in TaC_y perturbations from a lattice vacancy are longer ranged than in NbC_y. The data on the basic lattice parameter of disordered ($\eta = 0$) niobium and tantalum carbides were approximated by a second-degree polynomial $a(y, 0) = a_0 + a_1 y + a_2 y^2$ (for NbC_y the coefficients are $a_0 = 4.1004$ A, $a_1 = 0.7037$ A, and $a_2 = -0.3367$ A, and for TaC_y, $a_0 = 4.1630$ A, $a_1 = 0.4675$ A, and $a_2 = -0.1750$ A [74]).

Experimentally, the appearance of structural vacancies in disordered carbides is evident from the reduction in the lattice parameter. In the stoichiometric $MC_{1.00}$ carbide each metal atom forms localised M – C bonds with six nearest-neighbour carbon atoms, and partially localised M – M bonds with twelve metal atoms. In nonstoichiometric MC_y the presence of one or more vacancies in the first coordination sphere of a metal atom results in the atom being statically displaced, due to the asymmetry in the net influence of its nearest neighbours. The magnitude and direction of the displacements depend, to a first approximation, on the relation between E_{M-C} and E_{M-M} (the total energies of the respective nearest-neighbour M – C and M – M interactions the atom is involved in).

If $E_{M-M} > E_{M-C}$, the metal atoms surrounding a vacant site must come closer to one another. The compression of vacant octahedral interstitials $\square M_6$ will be hindered by the M – C interactions in the occupied neighbouring CM_6 octahedra. An increase in the concentration of vacant interstitials, which areas are smaller in size compared to those occupied, will reduce the lattice parameter provided the vacancy-produced static displacements of the metal atoms monotonically decrease and asymptotically vanish away from the vacancy. A reduction in lattice parameter will even occur if the perturbations from the vacancy spread only over the first coordination sphere.

If $E_{M-M} < E_{M-C}$, the nearest-neighbouring atom metals move away from the vacancy, and its linear size increases; hence for the lattice parameter to decrease, the metal atoms forming the vacancy's second coordination sphere must move towards it, i. e., the perturbation field of the vacancy must extend over at least two coordination spheres. For the MC_y carbides it is estimated [79, 80] that the effective perturbation radius is several times the unit cell period and that the perturbation extends farther than two coordination spheres. In this case the attenuation of perturbations away from the vacancy behaves like Friedel oscillations.

Thus an increase in the lattice parameter of a disordered carbide with vacancy concentration may involve either an increase or decrease in vacancy size.

According to Refs [36 – 42, 47 – 49] and to the neutron diffraction results of Ref. [74], niobium and tantalum carbides form M_6C_5 superstructures in the composition ranges $NbC_{0.81} - NbC_{0.88}$ and $TaC_{0.79} - TaC_{0.89}$. The process of ordering involves an increase in the basic lattice parameter of the carbides (Fig. 1). An earlier study [77] of the nonstoichiometric tantalum carbide in the $TaC_{0.81} - TaC_{0.89}$ range also shows an anomalous departure of the lattice parameter $a(y)$ from a quadratic dependence. Given the TaC_y preparation conditions used in the study, the anomalous change in the basic lattice parameter may be accounted for by a partial disordering of the tantalum carbide samples.

Disordering in $NbC_y \square_{1-y}$ and $TaC_y \square_{1-y}$ carbides is observed at a comparatively high vacancy concentration ($0.12 < 1 - y \leqslant 0.21$). At such concentrations the vacancy perturbation regions overlap and partially compensate one another. In an ordered carbide nearest-neighbour structural vacancies are absent, so the overlap is significantly less than in a disordered carbide. But then it is easily understood that a basic lattice parameter increase is only possible when metal atoms move away from the vacancy. In contrast, if they come closer, the basic lattice parameter of an ordered carbide should be less than in a disordered carbide.

Thus, an increase in the basic lattice parameter of ordered compared to disordered carbide and a reduction in carbide lattice parameter with increasing number of vacancies are experimentally observable only if the metal atoms forming the first coordination sphere of the vacancy move away from the vacancy and if the crystal lattice perturbations due to the vacancy extend over no less than two coordination spheres. This is consistent with the experimental data on the static displacement of metal atoms: in nonstoichiometric carbides of Ti, Zr, and Nb the metal atoms of the first coordination sphere move away from the vacancy [81, 82]; for NbC_y, it is shown [83] that the Nb atoms in the first coordination sphere

move away from the vacancy, and those in the second approach it.

Ref. [74] suggests a phenomenological model to analyse quantitatively the increase in basic lattice parameter upon ordering. In nonstoichiometric carbides with the basic $B1$ (NaCl)-type structure, each metal atom in the first coordination sphere has six sites of the nonmetal sublattice which can either be occupied by carbon atoms or be vacant. This allows one to represent a $B1$ (NaCl)-type crystal as a set of regular dodecahedron-shaped clusters. Each one of them contains a metal atom, which is at the centre, and six nonmetal lattice sites. Such clusters fill the entire volume of the crystal and account for all the lattice sites with no exception. Note that the cluster so chosen has the same shape as the Wigner–Seitz cell used in crystal physics as a translationally repeated volume element of a spatial lattice (in our case, this is the Wigner–Seitz cell of the fcc lattice).

Assuming that the cluster volume V_m depends only on the number of vacancies m in it and is independent of their arrangement, the crystal volume V in this model can be represented in the form

$$V = N \sum_{m=0}^{6} \lambda_m P_m(y, \eta) V_m , \tag{2}$$

where $P_m(y, \eta)$ is the probability of a cluster of m vacancies; $\lambda_m = C_6^m$ is the multiplicity of the m-configuration of the cluster; N is the number of sites in the metal sublattice. On the other hand, the volume of the crystal may be represented in terms of the basic lattice parameter $a(y)$ as $V = (N/4)\, a^3(y)$. From this, and given the composition dependence of the lattice parameter, $a(y) = a_0 + a_1 y + a_2 y^2$, Eqn (2) for a disordered carbide becomes

$$\sum_{m=0}^{6} \lambda_m P_m(y, 0) V_m = \frac{1}{4} (a_0 + a_1 y + a_2 y^2)^3 , \tag{3}$$

where $P_m(y, 0) = (1-y)^m y^{(6-m)}$ is the probability of formation of an m-vacancy cluster in the disordered crystal. The solution to Eqn (3) is an expression for the volume of the cluster,

$$V_m = \frac{1}{4} \sum_{k=m}^{6} A_{6-k} \frac{k!\,(6-m)!}{6!\,(k-m)!} , \tag{4}$$

where A_{6-k} are the coefficients of y^k on the right-hand side of Eqn (3).

Each cluster contributes to the total crystal volume with probability P_m. For equilibrium conditions, the probability of a cluster with a varying number of vacancies in a crystal with an arbitrary degree of order may be represented [8, 10, 52] in the form

$$P_m = \frac{1}{6} \left[(6-m)\, n_1^{(d)} (n_2^{(d)})^{(5-m)} (1 - n_2^{(d)})^m + m (1 - n_1^{(d)}) (n_2^{(d)})^{(6-m)} (1 - n_2^{(d)})^{(m-1)} \right] , \tag{5}$$

where $n_1^{(d)} = y - (5/6)\,\eta$ and $n_2^{(d)} = y + \eta/6$ are the respective probabilities for a carbon atom to occupy a site of the vacancy or carbon sublattice as the M_6C_5 superstructure is forming.

Using Eqns (2), (4), and (5), one can find the crystal volume and hence the basic lattice parameter for an MC_y carbide of any degree of order. Calculation of the basic lattice parameter of ordered carbide was carried out in two ways in Ref. [74]. In the first approach MC_y is taken to have the maximum lro η_{max}, which for M_6C_5 superstructures is

$$\eta_{max} = \begin{cases} 6(1-y), & \text{if } y \geqslant \dfrac{5}{6} , \\ \dfrac{6y}{5}, & \text{if } y < \dfrac{5}{6} . \end{cases} \tag{6}$$

The second approach assumes that the degree of order equals the lro parameter at the order–disorder phase transition. In other words, in the former case one sets $\eta = \eta_{max}$, and in the latter, $\eta = \eta_{tr}$ (the η_{tr} values were taken from Ref. [8]).

Table 3 for NbC_y and TaC_y lists the difference in the basic lattice parameter of the ordered versus disordered states, $\Delta a = a(y, \eta) - a(y, 0)$, both experimental and computed (in two different approximations). The data in the table show that the experimental Δa are fitted best with the approximation $\eta = \eta_{tr}$; hence, the niobium and tantalum carbides studied in Ref. [74] had reached the degree of lro characteristic of the thermodynamically equilibrium carbon and vacancy arrangement. The reduction of the experimental Δa in TaC_y compared to NbC_y is attributed to the fact that, under identical annealing conditions, the nonstoichiometric tantalum carbide cannot reach the same degree of order as niobium carbide can.

Physically, to fill the entire volume of the crystal lattice by Wigner–Seitz-cell clusters is possible when all the clusters have the same volume. In the model of Ref. [74] clusters with different number m of vacancies have a different volume V_m. The condition (2) is then fulfilled due to the cluster overlap regions being compensated by the regions where the faces of the neighbouring clusters do not touch. The presence of such regions implies that the nonmetal sublattice sites are split between neighbouring clusters and that the continuity of the medium breaks down. This can be remedied by using the

Table 3. Basic lattice parameter difference $\Delta a = a^{ord} - a^{disord}$ of the ordered and disordered MC_y carbides NbC_y and TaC_y [74].

y	Δa, A					
	NbC_y			TaC_y		
	Experiment	Calculation		Experiment	Calculation	
		$\eta = \eta_{trans}$	$\eta = \eta_{max}$		$\eta = \eta_{trans}$	$\eta = \eta_{max}$
0.78	—	0.0034	0.0087	—	0.0016	0.0044
0.80	0.0020	0.0038	0.0091	0.0007	0.0020	0.0047
0.83	0.0058	0.0045	0.0098	0.0045	0.0025	0.0053
0.86	0.0027	0.0040	0.0066	0.0021	0.0020	0.0034
0.88	0.0010	0.0031	0.0050	0.0010	0.0015	0.0024
0.90	—	0.0034	0.0021	—	0.0010	0.0017

Dirichlet–Voronoi polyhedron cluster, a distorted Wigner–Seitz cell with the amount of distortion depending on the number and mutual coordination of vacancies in the cluster and its nearest environment.

Note that the change in the lattice parameter of niobium and tantalum carbides as ordering proceeds, is quite comparable with lattice parameter changes within that part of carbide homogeneity regions where ordered phases form. For example, for a disordered niobium carbide in the region $NbC_{0.81}$ – $NbC_{0.88}$, the basic lattice parameter changes from 4.445 to 4.466 A, that is, by 0.021 A, whereas the minimum order-induced change in lattice parameter is 0.006 A. For a disordered tantalum carbide in the region $TaC_{0.81}$ – $TaC_{0.89}$, the respective figures are 0.014 A and 0.005 A. Thus, as to the order of magnitude, nonstoichiometry and ordering have a comparable effect on the basic lattice parameter in carbides.

The above analysis of the change in volume on M_6C_5 superstructure formation in niobium and tantalum carbides [74], together with the data on the effect of ordering on the basic lattice parameter in nonstoichiometric VC_y, NbC_y, and TaC_y [38 – 42, 67, 74], provide evidence that lattice parameter increases at the transition to an ordered state. The change in volume caused by the ordering or disordering process indicates that the disorder–order and order–disorder transitions considered here are first-order phase transitions. This fully agrees with experimental data [36, 38, 44 – 46, 67, 68] and symmetry analysis [12, 52, 63], and is also confirmed by order-parameter functional calculations [8, 20 – 24] which show the M_6C_5 and M_8C_7 superstructures to be formed by the first-order phase transition mechanism.

3. Electronic structure and spectroscopy of ordered carbides

One of the major methods for obtaining information about the electronic spectrum of a compound is the first-principles quantum mechanical calculation of its electronic states. For transition metal compounds, band calculations rely on the density-functional method and the local-density and atomic sphere approximations. The one-electron equations obtained in this way are solved self-consistently using the augmented-plane-wave method. For compounds of the heavy transition metals Hf and Ta, relativistic effects must be added [84].

To date, exact band calculations have only been carried out for vacancy-free stoichiometric carbides $MC_{1.00}$. It is found that the electronic density of states (DOS) at the Fermi level, $N(E_F)$, is different from zero and that the spatial distribution of electron concentration through the unit cell is such as to secure a metallic conduction and metal-metal interactions. Charge transfer from metal to nonmetal atoms gives rise to electrostatic interactions and is responsible for the ionic component of interatomic bonding. In addition to that, several types of bonding and antibonding covalent interactions exist. The most important of these are the metal *p*-nonmetal *d* bonds. A covalent metal–metal component is also present.

Thus, quantum mechanical calculations predict a combined covalent–metallic-ionic chemical bonding for *B*1 MC carbides. This is quite consistent with the observation that these compounds combine the basic properties of a metal (simple structure and a high conductivity decreasing with temperature) with those of covalent crystals (high hardness, brittleness, and low plasticity).

To calculate electronic spectra including nonstoichiometry (i. e., structural vacancies) requires by far less accurate approximations compared to the ideal defect free case: for example, the cluster approach or the ordered-structure translational-supercell scheme (the latter securing in a natural way the Born–Karman condition). The cluster approach is attractive in that it allows to model local defects, nonstoichiometry deviations, and lattice distortions while at the same time significantly reducing computations. However, modelling a solid by its small fragment runs into serious problems because of the need to include boundary conditions and to distinguish between the neighbourhood of an atom on the cluster surface and its real neighbourhood.

The virtual crystal approximation does not work for nonstoichiometric compounds because it is valid only as long as the defects have little influence on the spectrum and when the rigid band model is used. Within the band approximation framework, the most adequate approach is to employ the Korringa–Kohn–Rostoker (KKR) coherent-potential approximation within the LCAO (linear combination of atomic orbitals) scheme.

Using these approximations permits one to calculate the electronic spectrum for a carbide with either a single vacancy or a large concentration of ordered vacancies. To calculate the spectrum of a nonstoichiometric compound for any concentration of vacancies arbitrarily distributed in the lattice is not possible at present. However, it is this information which is necessary for and relevant to the interpretation of the properties of nonstoichiometric carbides.

Now how does the electronic spectrum change as more and more vacancies are introduced into an originally defect-free stoichiometric crystal? In other words, what is the change in the state of those electrons of metal atoms that are liberated from the metal–carbon bonds as a vacancy appears nearby? How do the conduction electrons alter their state; do metal–metal bonds pass through a vacancy form; what is the position of, and the electronic DOS at, the Fermi level; what is the electron concentration at the vacancy? Modern quantum mechanical analyses fail to give a clear answer to these questions.

At present it is considered established that the formation of a vacancy produces a narrow local peak in the conduction-band DOS 1 to 3 eV below the Fermi level, implying that the band does not remain rigid as vacancies are introduced and the electronic spectrum rearranges itself. Calculations show that the states forming the vacancy-related density peak are *d*-like, but the degree of their localisation has not been determined [85, 86]. It is also known that the appearance of vacancies in a carbide alters the relationship between the charges on the metal and carbon atoms and that an increase in vacancy concentration brings about a reduction in the atom-localised charge.

Since electronic spectrum calculations for nonstoichiometric compounds offer very limited possibilities at present, experimental methods for the study of the electronic structure are coming forward. Some features of the spectra can be determined by examining the electronic structure sensitive properties of the compounds.

3.1 X-ray emission and photoelectron spectra

Although electron spectroscopy is used widely for studying the electronic structure of nonstoichiometric carbides, little work has been done on carbides in the ordered state.

Ref. [87, 88] were concerned with the $L\beta_{2.15}$ and $L\gamma_1$ X-ray spectra in $NbC_{0.81}$, $NbC_{0.83}$, and $NbC_{0.88}$ in disordered and ordered states, and also in stoichiometric $NbC_{1.00}$ and disordered $NbC_{0.71}$.

A comparison of the Nb$L\beta_{2.15}$-spectra in NbC_y in ordered and disordered state (Fig. 2) reveals that the X-ray emission spectra of ordered carbide have a simpler form, with fine structure disappearing in the middle of the *C* emission band. This is indicative of the fewer types of positions (or of nearest-neighbour environments) available for Nb atoms in ordered versus disordered carbide, and is consistent with the NMR results on ordering in niobium carbide [38, 89, 90].

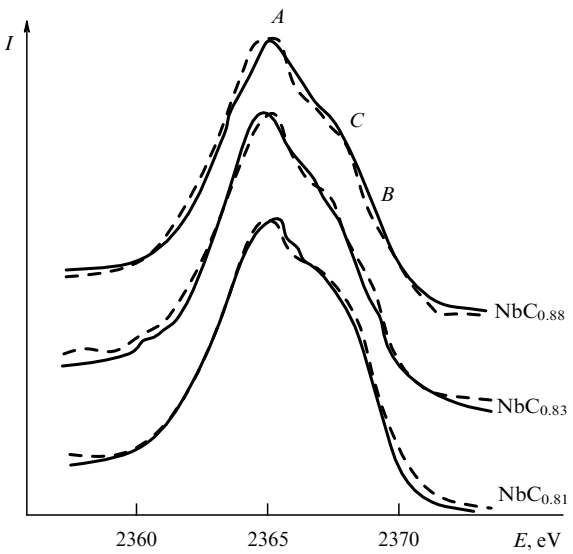

Figure 2. The X-ray emission Nb$L\beta_{2.15}$ spectra of the $NbC_{0.81}$, $NbC_{0.83}$ and $NbC_{0.88}$ carbides in disordered (solid line) and ordered (dashed line) states [87].

The maximum intensity of the high-energy *d*-like *B* band relative to the C2*p*-like *A* band is observed in $NbC_{0.71}$. The rise in *d* band intensity with decreasing carbon content implies an increased filling of the band. This is consistent with the result [91] that the growth of vacancy concentration in the carbon sublattice is accompanied by the filling of the *d* band. Also, as the concentration of structural vacancies is increased (from $NbC_{1.00}$ to $NbC_{0.71}$), the energy separation of the *A* and *B* bands decreases: from 3.3 to 1.9 eV in the $L\beta_{2.15}$ spectra and from 3.1 to 1.9 eV in $L\gamma_1$.

The influence of ordering on the Nb$L\gamma_1$ spectra, which reflect the distribution of Nb $4d_{3/2}$ states in the valence band, was studied for $NbC_{0.83}$, a carbide which corresponds to the stoichiometric composition of the ordered Nb_6C_5 phase. The ordering effect is stronger in the $L\gamma_1$ than in $L\beta_{2.15}$ spectra. Moving from the disordered to ordered $NbC_{0.83}$ leads to a marked decrease in the middle-part intensity of the $L\gamma_1$ spectrum *C* emission band and reduces from 3.5 to 2.4 eV the energy separation difference between the *A* and *B* subbands (Fig. 3).

Now what causes the changes in the X-ray emission spectrum observed as carbon atoms and vacancies are being ordered in a nonstoichiometric niobium carbide?

Cluster calculations show [92, 93] that the formation of a vacancy rises the Fermi level by about 0.19 eV in NbC_y; this is accompanied by a high degree of localisation of the electron

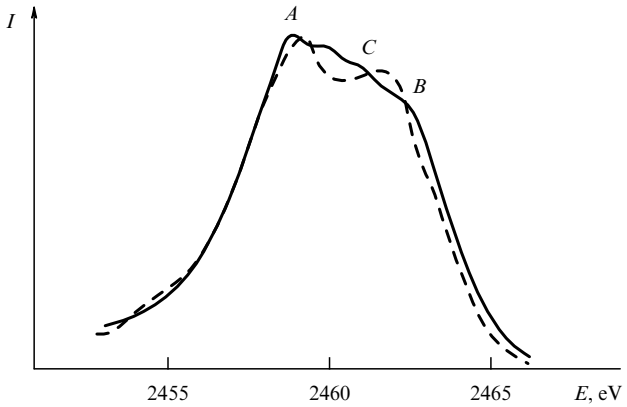

Figure 3. The X-ray emission Nb$L\gamma_1$ spectra of the $NbC_{0.83}$ carbide in disordered (solid line) and ordered (dashed line) states [87].

distribution perturbations introduced by single vacancies. The X-ray photoemission spectra of the $NbC_{0.89}$ and $NbC_{0.85}$ [94] show that on deviation from stoichiometry a new peak, one corresponding to vacancy states, appears below the Fermi energy. The maximum *B*, clearly distinct in the ordered $NbC_{0.83}$ spectrum (Fig. 3), is very much reminiscent of the vacancy-state peak observed in Ref. [94]. A local DOS peak due to vacancy formation is also suggested by niobium carbide superconductivity data [95].

However, the appearance of a vacancy in the nonmetal sublattice not only may produce vacancy states proper but can also split off some of the neighbouring metal *d* levels. According to Ref. [96], the emission *L* spectra of a transition metal in a compound is determined by the interaction of the *d* wave functions of the metal atom with those of its nearest-neighbouring atoms, so for each type of metal atom environment there is a corresponding spectrum with a certain amount of *d*-like *B* band/C2*p*-like *A* band splitting. This accounts rather simply for the difference in the *L* spectra of the disordered and ordered niobium carbides of the same composition.

In niobium carbide each Nb atom is within an octahedron of six nonmetal sublattice sites, some of which are probably vacant. In disordered NbC_y, there are all types of octahedral clusters, from the complete NbC_6 to fully defective Nb $\square_6$, but their probabilities of occurrence are different. In ordered carbide, the NMR and magnetic susceptibility data [38, 90, 97, 98] suggest that the most probable cluster type is $NbC_5\square$, with one vacancy and five carbons in the niobium nearest-neighbour environment.

If one assumes that X-ray *L* emission spectra depend on the metal atom nearest-neighbour environment and are superpositions of the contributions from different cluster types, then each one of the contributions must be proportional to the probability of occurrence of the corresponding cluster configuration in the crystal. Then the *L* spectra of disordered niobium carbide, to which all possible cluster configurations contribute, are more complex in form compared to ordered carbide, where only one cluster type, $NbC_5\square$, dominates. This is precisely the way the *L* spectra change upon ordering (Figs 2 and 3).

For nonstoichiometric TaC_y, the experimental and theoretical study of the electronic energy spectrum is very complicated compared to 3*d* and 4*d* transition metal carbides: X-ray emission spectroscopy is virtually impossible because

of the large (about 10 eV) width of the inner Ta levels [99], whereas theoretical quantum mechanical calculations require a detailed treatment of the relativistic effects due to the Ta *f* electrons. [86]. Consequently, the spectrum of disordered TaC_y was studied by X-ray photoelectron spectroscopy [85, 100 – 103].

Before discussing the results of these studies, let us dwell on the role of the C 2*s* electrons in valence band formation in carbides.

There is experimental evidence [85, 102, 103] for a band with an intensity peak approximately corresponding to the binding energy $E_b \approx 12$ eV as measured from the Fermi level. As carbon content is decreased in TaC_y, the band shifts slightly to the Fermi level and decreases in intensity [85]. It is shown [104 – 106] that the 12 eV band in tantalum carbide and similar bands (with somewhat different binding energies) in other transition metal carbides and nitrides correspond to the two nonmetal 2*s* (valence) electrons. Since the impurity states of metal valence electrons are a negligible fraction of nonmetal 2*s* states, it is expected that the carbon 2*s* electrons will take practically no part either in the covalent, or in metallic or ionic chemical bonding and so are not in fact valence electrons. Accordingly, the concept of binding electron concentration, $z = z_M + 2y$, have been introduced [100] for nonstoichiometric MC_y's, where z_M is 4 or 5 for the group-IV and -V transition metals, respectively, and the factor of 2 is the number of carbon electrons participating in chemical bonding in carbides. It is the binding electron concentration which determines changes in carbide properties in the homogeneity region.

Reference [100] focuses on the tantalum carbide energy bands corresponding to the chemical bonding electrons. In Fig. 4 the X-ray photoelectron spectra of the TaC_y and Ta valence bands are shown normalised to the integrated intensity of the Ta4*f*-spin doublet. The spectra are shown in a relative energy scale with zero taken to be the Fermi level of the respective sample. The spectra have four features, *A*, *B*, *C* and *D* (Fig. 4).

As carbide composition is varied from $TaC_{1.00}$ to $TaC_{0.79}$, the *A* band, with a maximum at about 5 eV, shifts by approximately 0.2 eV towards the Fermi level (Fig. 4). Earlier, a similar *A* band shift of 0.6 eV on moving from $TaC_{0.97}$ to $TaC_{0.52}$ had been found [85]. Analogous results (0.35-eV *A* band shift from $TaC_{1.00}$ to $TaC_{0.72}$) have been obtained in a non-self-consistent, relativistic KKR Green's function calculation [86].

While the position of the *B* band does not change with tantalum carbide composition (Fig. 4), its relative intensity increases with the concentration of structural vacancies [85, 86, 100].

The *C* band position changes from 2.7 eV for $TaC_{0.92}$ to 2.4 eV for $TaC_{0.79}$, its intensity increasing with the deviation from stoichiometry; in near-stoichiometric $TaC_{1.00}$ and $TaC_{0.96}$ the *C* band is essentially absent (Fig. 4). All X-ray photoelectron spectra of tantalum carbide exhibit a superposition of the *D* band [100, 102, 103].

Analysis of both the experimental [85, 100 – 103] and theoretical [86, 104 – 106] results on tantalum carbide electronic spectra shows that the *A* band reflects the state of the C2*p*- and Ta5*d*-electrons of the covalent M – C bonds, and the *B* band reflects the state of the M – M bond 5*d*-electrons. Despite the essentially nonfree nature of the M – M bond 5*d* electrons, they form a wide conduction band, their DOS function being a distorted Fermi distribution of the Ta *d* electrons (Fig. 4, spectrum 7). Against the background of the wide conduction band with intensity peak *B*, there is a much narrower covalent-electron band with an *A* peak. The *D* superposition can be interpreted as due to the narrow *A* band being superimposed on the wide conduction band.

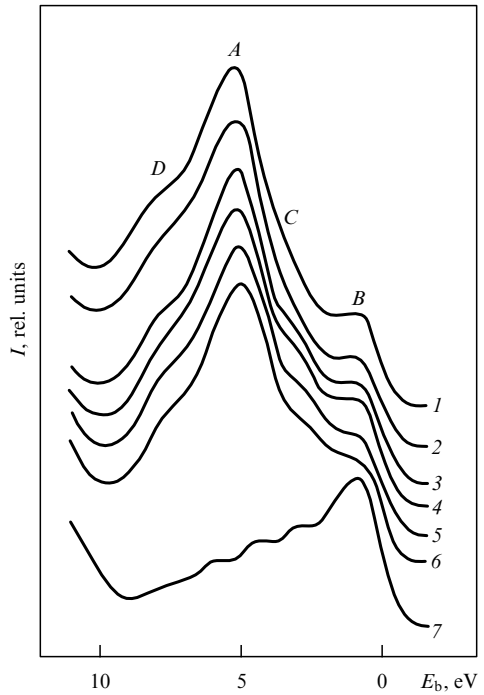

Figure 4. The X-ray photoelectron spectra of the valence bands of disordered carbides $TaC_{1.00}$ (*1*), $TaC_{0.96}$ (*2*), $TaC_{0.92}$ (*3*), $TaC_{0.90}$ (*4*), $TaC_{0.85}$ (*5*), $TaC_{0.79}$ (*6*), and metallic Ta (*7*), normalised to the integrated intensity of the Ta4*f* spin doublet [100].

The *C* band has a direct relation to the formation of vacancies in the carbide's metal sublattice. According to Ref. [86], the *C* band corresponds to the vacancy states of electrons of *p* symmetry. This is confirmed by there being no *C* peak in the X-ray photoelectron spectra of stoichiometric $TaC_{1.00}$ and near-stoichiometric $TaC_{0.96}$. Earlier [93], this peak was explained by the M – M bond electron states splitting off from the main *B* band under the vacancy-induced perturbation.

Figure 5 shows the variation with composition of the bonding energy of Ta4$f_{7/2}$ of the disordered *B*1 TaC_y in its homogeneity region (data from Refs [85, 100, 101, 103]). With the only exception of Ref. [101], the data invariably indicate an increase in the shift ΔE_b with carbon content. The most accurate — and closest — are the results of Refs [85] and [100], which can me approximated by the linear functions $E_b = 22.31 + 1.21y$ eV and $E_b = 21.96 + 1.65y$ eV, respectively.

An estimate of the effective charge $q_{Ta}(y)$ of Ta atoms in TaC_y was carried out in Ref. [100] by assuming a linear relation $\Delta E_b = kq$ [107] between the atomic charge q and the atomic inner level shift ΔE_b, to give $q_{Ta}(y) = 0.34 + 1.65y$ [e] [85] or $q_{Ta}(y) = 0.69 + 1.21y$ [e] [100]. This implies that for the stoichiometric $TaC_{1.00}$ the charge of a Ta atom is approximately +1.9 e and decreases with the concentration of structural vacancies.

The binding energy of the inner carbon C1*s* level is essentially composition independent, so to a first approxima-

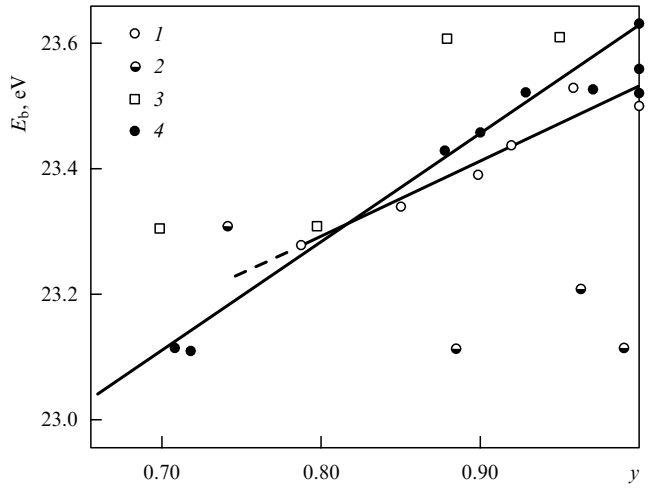

Figure 5. The binding energy of the inner level Ta4$f_{7/2}$ in disordered tantalum carbide TaC_y: *1*, Ref. [100], error in E_b is $\pm$ 0.03 eV; *2*, Ref. [101], error is $\pm$ 0.2 eV; *3*, Ref. [103], error is $\pm$0.1 eV; *4*, Ref. [85], error is not known. The results of Refs [85] and [100] are approximated by linear functions.

tion the charge of C atoms in a carbide does not depend on the concentration of structural vacancies. Since the charges of C and Ta atoms in stoichiometric $TaC_{1.00}$ are equal in absolute value, the charge of a C atom is $q_C \approx -1.9$ e. An estimate of the vacancy charge $q_\square$ using the obtained $q_{Ta}(y)$ and q_C values and the crystal's electrical neutrality condition $q_{Ta}(y) + yq_C + (1-y)\,q_\square = 0$ showed [100] that the vacancy charge is composition independent, negative, and equals -0.34 e [85] or -0.69 e [100]. The charge of a structural vacancy is much smaller in absolute value than that of Ta and C atoms. This means that it is metal and carbon atoms, not vacancies, that contribute most to the ionic component of chemical bonding in tantalum carbide.

3.2 Electron-positron annihilation

Electron-positron annihilation (EPA) is a promising method for the study of the electronic structure of substances with a perfect or imperfect lattice. In recent years the method has been widely used in the work on thermal and structural vacancies [108 – 112] and in studying vacancy clusters and radiation-induced pores [113]. The studies have shown the annihilation to be very sensitive to the vacancy content in a metal in the concentration range from 1×10^{-6} to 1×10^{-3} vacancies per atom.

Vacancy content in nonstoichiometric interstitial compounds (for example, in transition metal carbides) are two orders of magnitude above the EPA sensitivity limit established for metals. It should be kept in mind, however, that structural and thermal vacancies differ in their electronic properties [6, 7, 10]. This naturally raises the question of EPA applicability to nonstoichiometric compounds. Works [114 – 119] were the first to apply the method to the study of the electronic properties of nonstoichiometric carbides.

The objective of Ref. [116] was to determine the kinetic energy spectra of valence electrons in the group-IV and -V transition metals, in carbon (graphite) C, and in disordered cubic carbides MC_y of the same transition metals, using the angular correlation of annihilation radiation (ACAR) method. An attempt to compare the electronic states of pure metal and carbon with those in carbides was also made.

To obtain ACAR spectra, group-IV and -V transition metals (fcc Ti, Zr, and Hf, and bcc V, Nb, and Ta), and the carbides ($TiC_{0.94}$, $ZrC_{0.88}$, $HfC_{0.90}$, $VC_{0.85}$, $NbC_{0.93}$, and $TaC_{1.00}$) were used. Impurity content was nowhere above 1×10^{-3} at. percent. Prior to the experiment, metal plates were annealed at 1500 K for 6 hours and then slowly cooled to room temperature to release internal stresses and reduce the thermal vacancy content. The slow cooling made it possible to ignore the positron trapping by thermal vacancies. The reactor graphite used had the hexagonal structure $P6_3/mmc$ with impurity content of no more than 1×10^{-4} at. percent.

The results of Ref. [116] for metals compare favourably with the earlier data, for example for annealed Ta [121] and non-irradiated V and Nb [120]. However, later work [121] yielded Ta ACAR spectra very different from those of Refs [108] and [116], presumably due to the impurities present in tantalum investigated in Ref. [121].

That the ACAR spectra of carbides and transition metals obtained in Ref. [116] are qualitatively close indicates the similarity in their electronic structure. Quantitative differences in the spectra of various carbides are beyond experimental error, which made it possible to examine electronic structure as a function of the transition metal type.

In the literature, the ACAR spectra are most commonly approximated by a superposition of a Gaussian and a truncated inverted parabola [122, 123]. For normal metals, this picture has a straightforward explanation which enables a theoretical analysis of experimental data. The Gaussian corresponds to the contribution from the positron annihilation with core electrons, whereas the parabola accounts for annihilation at conduction electrons. For the transition metals and their compounds, this explanation is complicated by band hybridisation near the Fermi level.

In nonstoichiometric carbides a thermalised positron may be found either in a free (Bloch) or a bound state, in which latter case it may be trapped at either a nonmetal or metal structural vacancy. Thus, in nonstoichiometric carbides (as opposed to metals) a positron may annihilate from three states, one free and two bound. The concentration of metal vacancies in the carbides studied was reduced to a minimum by annealing followed by a slow cooling to room temperature; also, the charge of a carbon vacancy in a carbide is significantly less than a vacancy charge in a metal. So to a first approximation, only free-state positron annihilation may be considered [115, 116].

In metals, at a certain concentration of defects (thermal or radiation-induced vacancies) electron-positron annihilation parameters tend to saturate, i. e., remain unchanged as vacancy content is increased further [113, 124]. This concentration varies widely but does not exceed 1×10^{-3} vacancies per atom. As the saturation is approached, the vacancy concentration in a metal turns out to be sufficient to trap all positrons, but is too low for the vacancies to affect one another, i. e., for their electronic characteristic to be concentration dependent. The situation in nonstoichiometric carbides is somewhat different. The concentration of structural vacancies may reach 0.25 per atom. At such a high concentration, vacancy interaction is inevitable and hence so is the variation of their electronic characteristics with concentration.

Because of the Coulomb repulsion from the nuclei, a positron in a crystal tends to annihilate in the inter-core space. In the transition metals, however, the annihilation involves not only conduction electrons but also those of the partially

filled d shells [125]. Nonstoichiometric transition metal carbides possess metallic conductivity, and in their intercore space there are both hybridised sp conduction electrons and electrons that form covalent bonds (metal d and nonmetal p electrons), the covalent d and p electrons having much higher concentration than the conduction electrons. Clearly, in transition metal carbides the probability of annihilation with core electrons is negligible. Accordingly, it was assumed [115] that in nonstoichiometric carbides the free state annihilation involves conduction electrons and covalent-bonding electrons, and therefore two contributions to the positron annihilation spectrum are considered.

Assuming the conduction electrons to be free, the authors of Refs [122, 126] obtain the following expression for the intensity of the angular correlation curve for annihilation γ quanta:

$$I_{\mathrm{p}}(\theta) = h_{\mathrm{p}}\left[1 - \left(\frac{\theta}{\theta_{\mathrm{p}}}\right)^2\right] f\big(|\theta| - \theta_{\mathrm{p}}\big)\,, \tag{7}$$

where

$$f\big(|\theta| - \theta_{\mathrm{p}}\big) = \begin{cases} 1, & \text{or} \quad |\theta| \leqslant \theta_{\mathrm{p}}\,, \\ 0, & \text{or} \quad |\theta| > \theta_{\mathrm{p}} \end{cases}$$

is the Heaviside function. The expression (7) describes an inverted parabola of height h_{p} with cut-off angle θ_{p} (the angle where I_{p} vanishes).

As for the second contribution, it has been shown empirically [122] that in transition metals it can be approximated by the Gaussian distribution

$$I_{\mathrm{g}}(\theta) = h_{\mathrm{g}} \exp\left(-\frac{\theta^2}{2\theta_{\mathrm{g}}^2}\right), \tag{8}$$

where h_{g} and θ_{g} are its height and half-width, respectively. Equation (8) describes the free positron annihilation with the valence d electrons (in metals) or with the covalent M – C bond electrons (in carbides).

From the above, the angular correlation curves for the nonstoichiometric carbides can be represented as a sum of two terms,

$$I(\theta) = I_{\mathrm{g}}(\theta) + I_{\mathrm{p}}(\theta)\,. \tag{9}$$

The experimental angular correlation function for annihilation radiation, $N(\theta)$, introducing the spectrometer angular resolution function $R(\theta)$, can be represented in the form

$$N(\theta) = \int_{-\infty}^{\infty} R(\theta' - \theta)\, I(\theta')\, \mathrm{d}\theta'\,. \tag{10}$$

The dependence (10) is described by the parameters h_{g}, θ_{g}, h_{p}, and θ_{p}, which were determined from experimental ACAR spectra in Refs [115, 116].

Fig. 6 shows, as an example, the experimental $N(\theta)$ and computed $I(\theta)$ angular correlation functions for nonstoichiometric $TaC_{1.00}$; a decomposition of the latter function into a Gaussian and a truncated parabola is also shown. Estimating the quality of approximation from the χ^2/ν criterion [127] shows that the function (10) provides a good quantitative description of the experimental ACAR spectra of carbides. An attempt to approximate the spectra by one or two Gaussians led to much larger disagreement between experiment and theory. On the other hand, improvements using three or more components (for example, a parabola and two Gaussians, etc.) proved to be statistically insignificant. Thus,

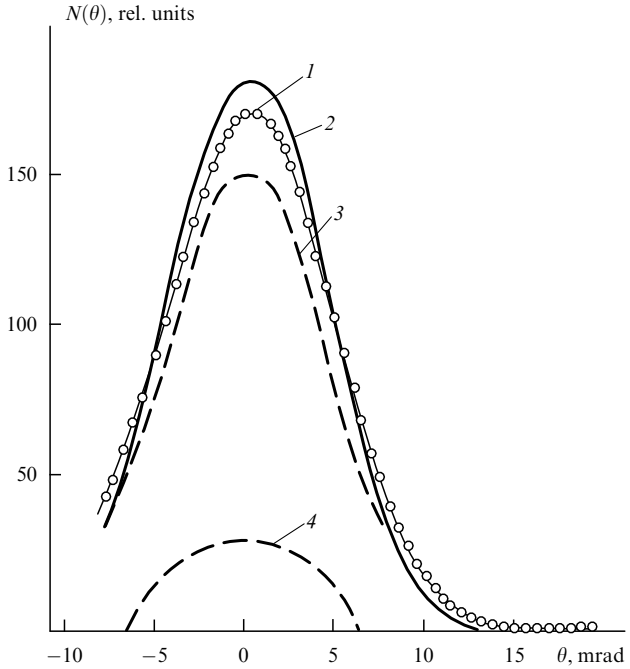

Figure 6. Components of the ACAR spectrum of $TaC_{1.00}$: *1*, experimental spectrum; *2*, restored true spectrum; *3*, Gaussian component; *4*, parabolic component [115].

statistical analysis shows that experimental ACAR spectra of nonstoichiometric carbides are described best by a parabolic and a Gaussian component [115, 116]. Table 4 lists the calculated parameters h_{g}, θ_{g}, h_{p}, θ_{p} and ratios $S_{\mathrm{p}}/S_{\mathrm{g}}$ for the carbides studied ($S_{\mathrm{g}} = h_{\mathrm{g}}\theta_{\mathrm{g}}\sqrt{\pi/2}$ is the area under the Gaussian curve, and $S_{\mathrm{p}} = 2h_{\mathrm{p}}\theta_{\mathrm{p}}/3$, that under the truncated parabola).

Fig. 7 shows the ACAR spectra of $NbC_{0.93}$ (*1*), niobium (*2*), and graphite (*3*). The qualitative relation between the ACAR spectra of a metal and its carbide is the same for other metals studied in Ref. [116]. The ACAR curves of the carbides lie between those for the metal and graphite. The implication is that the electronic structure of the carbides is not formed by the metal atoms alone: carbon atoms also contribute to the spectrum formation process.

For the more detailed discussion of the experimental data on positron annihilation in carbides, Ref. [115] modifies the free-state positron analysis by changing from electron angular spectra to electron momentum and energy spectra.

According to Ref. [115], the electron momentum density distribution has the from

$$\rho(p) = 4\pi\,(m_0 c)^2\, A^{-1} p^2 \times \left[\frac{2h_{\mathrm{p}}}{p_{\mathrm{p}}^2} f(|\mathbf{p}| - p_{\mathrm{p}}) + \frac{h_{\mathrm{g}}}{p_{\mathrm{g}}^2} \exp\left(-\frac{p^2}{2p_{\mathrm{g}}^2}\right)\right], \tag{11}$$

where A is the normalisation factor; $p_{\mathrm{g}} = m_0 c\theta_{\mathrm{g}}$ and $p_{\mathrm{p}} = m_0 c\theta_{\mathrm{p}}$ (m_0 is the free-electron mass, and c is the velocity of light). From (11) one can change to the electron kinetic energy distribution $\rho(E_{\mathrm{k}})$. For the conduction electrons the dependence of the DOS on E_{k} has the familiar form

$$\rho_{\mathrm{p}}(E_{\mathrm{k}}) = 2\pi\,(m_0 c)^2 \sqrt{2m_0}\, A^{-1} \sqrt{E_{\mathrm{k}}}\; \frac{2h_{\mathrm{p}}}{E_{\mathrm{p}}} f(E_{\mathrm{k}} - E_{\mathrm{p}})\,, \tag{12}$$

Table 4. Characteristics of the ACAR and kinetic spectra of valence electrons in transition metal carbides [115, 116].

Composition	Gaussian halfwidth θ_g	Parabola cut-off angle θ_p	Parabola height h_p	Gaussian height h_g	Area ratio S_p/S_g	Fermi energy E_F	Covalent band width ΔE_g
	mrad			rel. units		eV	
$TiC_{0.94}$	4.6	6.6	59	130	0.35	11	19
$ZrC_{0.88}$	4.2	6.4	61	140	0.36	10	16
$HfC_{0.90}$	4.5	6.3	80	116	0.51	10	19
$VC_{0.85}$	4.8	6.7	45	134	0.25	11	21
$NbC_{0.93}$	4.5	7.1	40	145	0.23	13	18
$TaC_{1.00}$	4.5	7.0	30	152	0.16	12	19
$TaC_{0.92}$	4.6	6.9	50	133	0.30	12	19
$TaC_{0.85}$ ordered	4.7	7.1	58	123	0.38	13	20
$TaC_{0.85}$ disordered	4.8	7.6	64	112	0.48	15	21
error	±0.05	±0.10	±5	±8	±0.01	±1	±1

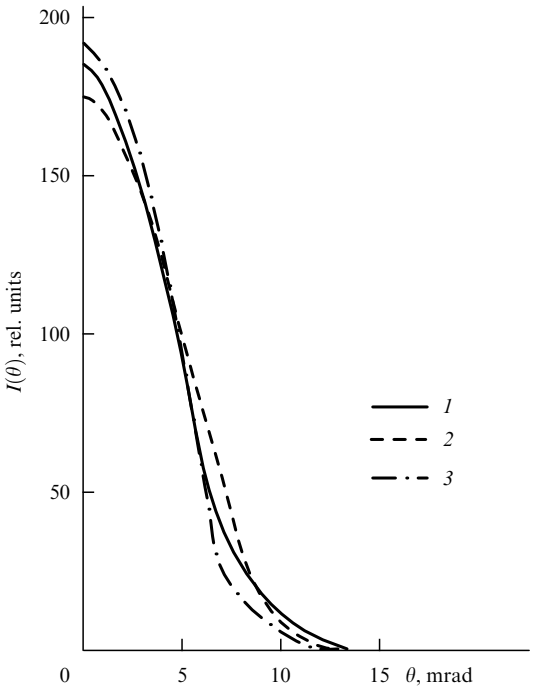

Figure 7. ACAR spectra of $NbC_{0.83}$ (solid line), metallic Nb (dashed line), and graphite C (dash dot line) [116].

and for the covalent-bonding electrons this dependence was written in the form

$$\rho_g(E_k) = 2\pi\,(m_0c)^2\sqrt{2m_0}\,A^{-1}\sqrt{E_k}\,\frac{h_g}{E_g}\exp\left(-\frac{E_k}{2E_g}\right), \tag{13}$$

where $E_p = m_0c^2\theta_p^2/2$ and $E_g = m_0c^2\theta_g^2/2$. We note that adding the expressions (12) and (13) directly is not physically meaningful because this neglects the fact that different electronic subsystems have different potential energies.

From Eqn (12) it is clear that the quantity E_p, as the maximum energy of conduction electrons, is in fact the Fermi energy E_F. According to Ref. [115], the energy band width of the covalent electrons is $\Delta E_g \approx 3.6E_g$. Table 4 presents the E_F and ΔE_g values calculated with the use of the θ_p and θ_g parameters known for carbides.

Comparison of the predicted S_p/S_g and E_F reveals a marked difference between the group-IV ($M^{IV}C_y$) and group-V ($M^{V}C_y$) transition metal carbides (Table 4). In $M^{V}C_y$ carbides the Fermi energy on the average is by 1 – 2 eV larger than in $M^{IV}C_y$, which compares qualitatively with quantum mechanical KKR results [128, 129], and is in quantitative agreement with X-ray emission data on zirconium and niobium carbides [130]. The rise in the Fermi energy from the group-IV to group-V carbide is, as indicated by calculations [128, 129], due to the filling of the metal–metal band by an additional d electron. On the other hand, for $M^{V}C_y$ carbides S_p/S_g is 1.5 to 2 times less than for $M^{IV}C_y$, although one would expect it to be larger due to the extra electron. The model of Ref. [116] does not clarify this point.

Of particular interest are the EPR data on the TaC_y in disordered and ordered states [114, 115]. The carbides studied were $TaC_{0.85}$ and $TaC_{0.79}$ in ordered and quenched states, and disordered TaC_y ($y = 1.00, 0.96, 0.92, 0.90$).

Approximating the experimental ACAR spectra by the function (10) enabled the parameters h_p, θ_p, h_g, θ_g, and S_p/S_g to be calculated for carbides TaC_y. The calculation showed that the ACAR spectrum parameters of nonstoichiometric TaC_y depend rather weakly on the content of structural vacancies, and that increasing their concentration does not lead to any significant narrowing of the angular correlation curves, as is the case for other types of defect [113]. Besides the weak composition dependence of TaC_y spectra, Ref. [115] also reports a marked difference between the spectra of ordered and disordered $TaC_{0.85}$. This suggests that the electron-positron annihilation parameters are order-sensitive.

The most pronounced changes found in the positron annihilation experiment on TaC_y [115] are those in the parameter S_p/S_g, which is proportional to the conduction electron concentration in the crystal. As composition changes from $TaC_{1.00}$ to $TaC_{0.79}$, the ratio S_p/S_g increases about twofold. Thus, positron annihilation data indicate that the conduction electron concentration grows as carbon content decreases in TaC_y. Similarly, from the data on S_p/S_g, the conduction electron concentration in quenched disordered $TaC_{0.85}$ is larger than in ordered. This is presumably due to the fact that the Fermi energy increases and the covalent

electron DOS decreases, upon ordering. Since the total number of electrons in TaC_y does not change on ordering, the higher concentration of conduction electrons in disordered compared to ordered carbide indicates that electrons are redistributed between the metallic and covalent chemical bonding components during the vacancy ordering process.

According to Ref. [122], the cut-off angle of the parabola mentioned above characterises the Fermi momentum of the conduction electrons. Analysis of the parameter θ_p showed that, within the accuracy of the experiment, E_F does not change with the composition of TaC_y. The average Fermi energy of carbides of various composition (except for disordered $TaC_{0.85}$) is 12 – 13 eV. The quenching-produced vacancy disordering in $TaC_{0.85}$ increases E_F by about 1 – 2 eV. The energy band width of covalent electrons is almost independent of TaC_y composition and equals 19 – 20 eV. For disordered $TaC_{0.85}$, the width $\Delta E_g \approx 21$ eV and is greater than for the ordered carbide of the same composition.

References [114 – 116] explain carbide ACAR data by assuming free state positron annihilation. A strong argument in favour of this assumption is that a good approximation to the spectra can only be achieved by including the parabolic component. In metals the parabolic ACAR component corresponds to the annihilation of positrons from a free state on conduction electrons. A second experimental argument in favour of free positron annihilation is the dependence of the annihilation parameters on vacancy concentration in nonstoichiometric TaC_y: the insaturability of the annihilation parameters implies that positrons are not trapped at the vacancies. However, the concentration of structural vacancies in the investigated tantalum carbides is very high (from 10^{-2} at. % of nonmetal vacancies in the very-near-stoichiometric $TaC_{1.00}$ to 21 at. % in $TaC_{0.79}$), and is sufficient to trap all positrons available. Also, the $c_\square$ dependence of annihilation parameters observed in Ref. [115] is very weak and may be due to positron trapping by vacancies provided changing $c_\square$ alters the electronic properties of a vacancy. Thus, the ACAR data [115] do not allow to say unambiguously whether a positron annihilates from a free state or whether it is first trapped by a vacancy and then annihilates from a bound one.

ACAR studies in carbides [114 – 116] showed the spectra to be weakly sensitive to the concentration of structural vacancies in the carbon sublattice. The observed weak changes of annihilation parameters are presumably due to the variation of the electronic properties of a structural vacancy with vacancy concentration. The spectra turned out to be sensitive to the structural (order–disorder) state of the carbides. Given the data on positron trapping by vacancies [17, 118], the model (9) can only be useful for estimating ACAR spectrum parameters but not for the physical interpretation of the results, and the presence of the parabolic ACAR component requires a theoretical understanding of both bound positron annihilation and the energy and spatial distribution of electron concentration in a vacancy.

Studies of the lifetime of positrons in carbides, τ_{MC_y}, have shown [117 – 119] that positrons are trapped by structural vacancies and annihilate from the bound (localised) state. The measurements were performed on the near-stoichiometric carbides $TiC_{1.00}$, $ZrC_{0.98}$, $HfC_{1.00}$, $NbC_{1.00}$ and $TaC_{0.99}$. Also investigated was the effect of the concentration of structural vacancies $c_\square$ on τ_{MC_y} in nonstoichiometric NbC_y ($0.72 < y < 1.00$) samples over the entire homogeneity region of the disordered phase.

Analysis of the experimental spectra showed them to be best fitted by a single exponential component. An attempt to employ two components with different positron lifetimes yielded a poorer convergence. This means that positron annihilation in carbides involves one type of defect only.

The positron lifetime τ in group-IV carbides is 160–176 ps, and in group-V carbides 155–161 ps. As the composition changes from $NbC_{1.00}$ to $NbC_{0.72}$, i. e., the concentration of structural vacancies rises from the minimal to maximal value, τ decreases from 161 to 151 ps. The positron lifetime in NbC_y and TaC_y is markedly (by about 40 ps) longer than in Nb and Ta. For TiC_y, ZrC_y, HfC_y, and corresponding group-IV metals, the lifetime difference is by far smaller (about 10 ps).

The analysis of the data from Refs [117, 118] showed that the normalised positron annihilation rate $\lambda^* = (\lambda - \lambda_\infty)/\lambda_\infty$ ($\lambda_\infty = 2.004 \times 10^9$ s^{-1}, $\lambda = 1/\tau$) does not correlate with the total electron concentration in metals and their carbides. This suggests that not all electrons contribute equally to positron annihilation in these substances. Presumably, positrons mostly annihilate with those electrons having sufficiently high concentration away from the positively charge nuclei.

In Fig. 8 the positron annihilation rate λ^* is shown as a function of the valence electron concentration $\eta^{val} = zV_B/V$, where z is the number of annihilating valence electrons that corresponds to the substance formula unit of volume V; $V_B = 6.208 \times 10^{-31}$ m^3 is the volume of a sphere of Bohr radius. The points around the straight line *1* correspond to the dependence of λ^* in $TiC_{1.00}$, $ZrC_{0.98}$, $HfC_{1.00}$, $NbC_{1.00}$ and $TaC_{0.99}$ on the total valence electron concentration (the total number of bonding electrons z in MC_y is $z = z_M + 2y$, where z_M is 4 or 5 for group-IV and -V transition metals, respectively [100]). The points around the straight line *2* give the dependence of λ^* in Ti, Zr, Hf, Nb, and Ta, and their carbides $TiC_{1.00}$, $ZrC_{0.98}$, $HfC_{1.00}$, $NbC_{1.00}$, and $TaC_{0.99}$ on the metal-atom valence electron concentration $\eta_M^{val} = z_M V_B/V$.

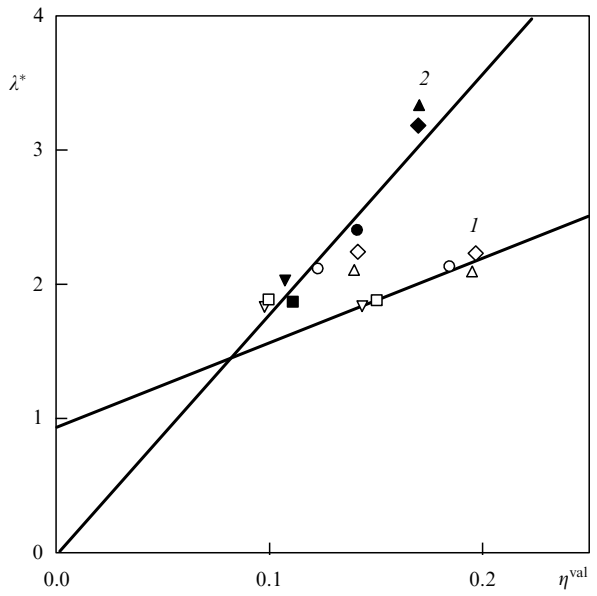

Figure 8. The dependence of the annihilation rate of positrons λ^* on the valence electron concentration η^{val}: *1*, λ^* (η_{tot}^{val}) for $TiC_{1.00}$ (○), $ZrC_{0.98}$ (▽), $HfC_{1.00}$ (□), $NbC_{1.00}$ (△) and $TaC_{0.99}$ (◇); *2*, λ^* (η_M^{val}) for Ti (●), Zr (▼), Hf (■), Nb (▲), Ta (◆), and their carbides [117, 118].

The experimental values of λ^* as a function of $\eta_{\rm tot}^{\rm val}$ for the carbides studied in Refs [117, 118] fall close to the curve *1* (Fig. 8), indicative of the positron annihilation at valence electrons, but are below the similar dependence well-known for metals [131]. Also, the curve *1* does not pass through the origin. This implies that not all valence electrons participate in annihilation.

The straight line *2*, which does pass through the origin, is drawn through the experimental points under the assumption that positrons in the carbides (and, naturally, in the metals) annihilate only with the metal-atom valence electrons. This experimental line $\lambda^* = 17.9\,\eta_{\rm M}^{\rm val}$ is close to that known for metals [131].

That positrons annihilate only with the metal-atom valence electrons and do not with the carbon-atom electrons is confirmed in Ref. [117] by the linear dependences of λ^* on $V_{\rm M}^{-1}$ ($V_{\rm M}$ is the volume per metal atom) constructed for the carbides of group-IV and -V transition metals.

A similar conclusion was drawn from the data on the concentration dependence of positron lifetime in nonstoichiometric niobium carbide. This decreases with the concentration of structural vacancies $c_\square = 1 - y$. The rise in $c_\square$ is accompanied by a decrease in the metal sublattice parameter a_{B1}, i. e., a compression of the lattice and a reduction in the volume $V_{\rm M} = a_{B1}^3/4$. The $\tau(V_{\rm M})$ dependence is linear within experimental error (Fig. 9). To a lower volume $V_{\rm M}$ there corresponds a shorter lifetime τ, i. e., with increasing nonstoichiometry the concentration of electrons for positron annihilation increases monotonically. This is possible if it annihilates only with the metal atom electrons. If carbon electrons were involved, the $\tau(V_{\rm M})$ dependence (Fig. 9) would have a different sense of slope, since the valence electron concentration $\eta_{\rm tot}^{\rm val}$ decreases with the concentration of structural vacancies. Thus, the investigation of nonstoichiometric carbides in Refs [117, 118] shows that positrons annihilate only with the metal-atom valence electrons, irrespective of the type of the metal and the carbon content.

The calculation of the lifetime of nonlocalised positrons $\tau_{{\rm MC}_y}^{\rm f}$ in carbides using a formula from Ref. [131] showed the lifetime to be shorter than in the respective metals: 105–115 ps for close-to- stoichiometric titanium, niobium, and tantalum carbides, and 125 – 135 ps for zirconium and hafnium carbides.

The positron lifetime in a metal vacancy $\tau_{{\rm MC}_y}^{\rm M\square}$ must be much longer because the first coordination sphere of the vacancy is formed by carbon atoms and carbon vacancies. The positron lifetime in a carbon vacancy $\tau_{{\rm MC}_y}^{\rm C\square}$ is expected to be between $\tau_{{\rm MC}_y}^{\rm f}$ and $\tau_{{\rm MC}_y}^{\rm M\square}$, since such a vacancy is surrounded only by metal atoms.

The carbide positron lifetimes measured in Ref. [118] are markedly longer than $\tau_{{\rm MC}_y}^{\rm f}$ and shorter than the $\tau_{{\rm MC}_y}^{\rm M\square}$'s computed in Ref. [132], and correspond to positrons localised on carbon sublattice vacancies. Further evidence for such a localisation comes from an annihilation experiment on carbides irradiated by high-energy electrons at 77 – 84 K [119]. The electron energy of 2.5 MeV was sufficient for the formation of metal vacancies [133 – 135], and the lifetime $\tau_{{\rm MC}_y}^{\rm M\square}$ of vacancy-trapped positrons must have been 170–180 ps. Within the accuracy of the experiment (± 2 ps), the measured positron lifetime in $TiC_{0.99}$, $NbC_{0.98}$, $NbC_{0.84}$, and $TaC_{0.99}$ is the same prior to and after irradiation and much less than $\tau_{{\rm MC}_y}^{\rm M\square}$. This means that positron annihilation in irradiated carbides also occurs at carbon vacancies. Presumably, the radiation-induced defects recombine just at the irradiation temperature, 80 K, leaving no metal vacancies in the irradiated carbides.

According to Ref. [119], the lifetime τ in disordered $NbC_{0.84}$ (a composition close to the perfectly ordered Nb_6C_5 phase) is about 10 ps longer than in the disordered carbide of the same composition (Fig. 10). On warming a disordered niobium carbide, τ remains unchanged to 900 K and then decreases because of disordering. In fact, for $NbC_{0.84}$ the temperature interval 1100 – 1300 K is the two-phase region where the ordered and disordered phases coexist [8, 20 – 22]. The decrease in τ upon $NbC_{0.84}$ disordering is consistent with the $\tau(V_{\rm M})$ dependence in Fig. 9, since the disordering of the carbide involves a lattice parameter decrease [10, 52, 74].

In Ref. [132] an LMTO-ASA calculation of the electronic structure and positron lifetimes for a number of *B*1 carbides is presented. A nonstoichiometric carbide is modelled by a cubic unit cell cluster, with four sites from each metal and nonmetal sublattice, and the vacant site at the centre. Such a cluster allowed modelling $MC_{0.75}$ (M_4C_3) or $M_{0.75}C$ (M_3C_4) with

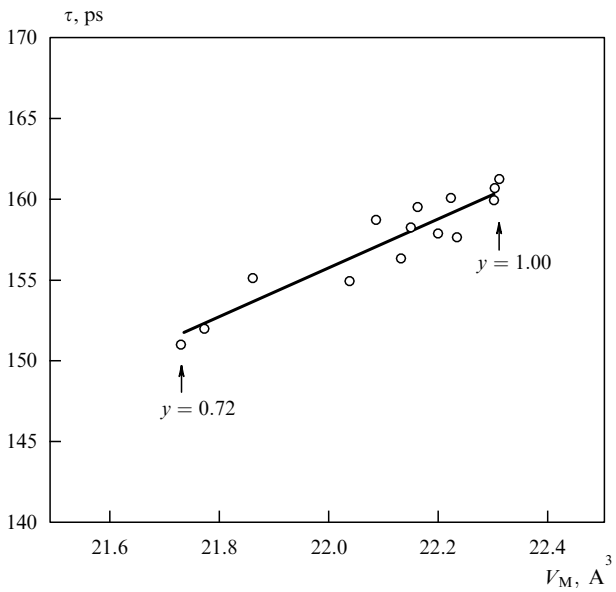

Figure 9. The dependence of the positron lifetime τ in NbC_y ($0.72 < y < 1.00$) on the volume $V_{\rm M}$ per metal atom [118].

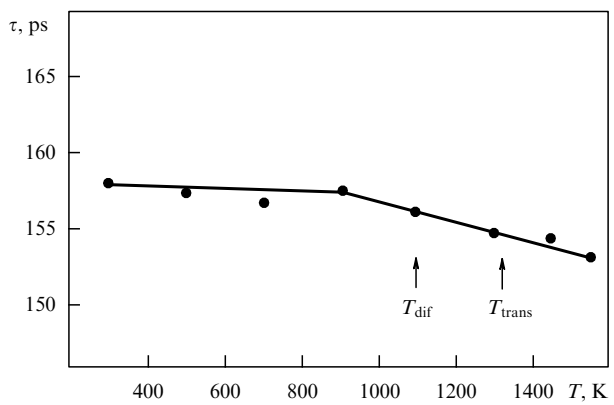

Figure 10. The change in the positron lifetime τ due to the heating and disordering of ordered $NbC_{0.84}$ ($T_{\rm dif}$ is the starting temperature for carbon diffusion and structural vacancy migration in the nonmetal sublattice; $T_{\rm trans}$ is the order–disorder transition temperature for $NbC_{0.84}$) [119].

25 at. percent of vacancies in the carbon and metal sublattices, respectively. A comparison of calculations [132] with measurements [117, 118] shows that the experimental τ are smaller than $\tau_{MC_y}^{M\square}$ and larger than $\tau_{MC_y}^{C\square}$, the predicted lifetimes in a metal vacancy (in M_3C_4) and in a carbon vacancy (in M_4C_3), respectively. Using this result, Ref. [132] assumes that the experimentally measured positron lifetime is the mean of $\tau_{MC_y}^{M\square}$ and $\tau_{MC_y}^{C\square}$. This conclusion is incorrect because the averaging of τ has no physical meaning at all: the annihilation of positrons at two types of defect would produce two components with different values of τ in the experimental spectrum. In addition, even a formal averaging of τ must include the vacancy concentration and take into account the difference in positron affinity for a metal and a carbon vacancy.

The discrepancies between experiment and calculation are due to the fact that in modelling high vacancy concentration $c_\square$ (25 at. percent) Ref. [132] ignores the interatomic spacing which change results from the introduction of vacancies. In fact, in calculating $MC_{0.75}$ and $M_{0.75}C$ these authors made use of the spacings determined for a perfect defect free $MC_{1,00}$, themselves substantially different from the experimental values; and this when the lifetime depends sensitively on the spacing. It would seem that Ref. [132] yields a correct qualitative relation between the positron lifetimes in metal, τ_M^f, and in carbon ($\tau_{MC_y}^{C\square}$) and metal ($\tau_{MC_y}^{M\square}$) vacancies in a carbide ($\tau_{MC_y}^{M\square} > \tau_{MC_y}^{C\square} > \tau_M^f$), but specific predictions for τ should only be considered as rough estimates.

Basically, the electron-positron annihilation data suggest that in nonstoichiometric carbides positrons are trapped by the vacancies in the carbon sublattice, the electronic properties of the vacancies depending on vacancy concentration. Thus, the EPA method is capable of giving information about a structural vacancy and the manner its properties change with the composition of a nonstoichiometric compound.

4. Effect of ordering on the properties of carbides

4.1 Electrokinetic properties

Nonstoichiometric carbides MC_y realise a combined covalent-metallic-ionic type of chemical bonding, the first two components being of comparable strength and the third, relatively weak. The electrical conductivity and other kinetic properties are determined primarily by the collectivised metal *d* electrons participating in M – M bonds.

In nonstoichiometric *B*1 (NaCl) carbides all of the nearest-neighbouring metal atoms lie in $(111)_{B1}$ (or equivalent $(11\bar{1})_{B1}$, $(1\bar{1}1)_{B1}$, and $(1\bar{1}\bar{1})_{B1}$) planes producing a close hexagonal packing in them. This suggests that conduction electrons are distributed non-uniformly over the crystal volume, showing concentration peaks near the close-packing metal planes [10]. Due to the metal and nonmetal planes alternating in the $[111]_{B1}$ and equivalent directions in the compounds under study, the conduction electrons propagate within a certain spatial grid formed by the close-packed metal planes. The nonmetal planes may be complete (no structural vacancies) or defective (vacancies along with carbon atoms), depending on the MC_y composition. Analysis of electrical-resistivity and other electrokinetic studies, which show the electrons to be strongly scattered by vacancies, suggests that the electron mean free path along metal planes depends on which nonmetal planes (complete or defective) are joined by metal atomic planes. In Ref. [10] it is assumed that the conduction electron mean free path is larger when a metal plane is between complete nonmetal planes and smaller otherwise. This enables the model of 2D conduction electron distribution to be used in discussing the electrokinetic properties of nonstoichiometric carbides.

Ordering in nonstoichiometric interstitial compounds leads to such a rearrangement of nonmetal atoms and structural vacancies which gives rise to complete and ordered nonmetal defective planes alternating in a certain fashion in the lattice [12]. In disordered nonstoichiometric compounds the nonmetal atomic planes are all defective. Given this difference between ordered and disordered nonstoichiometric compounds, the two-dimensional distribution model predicts that, all other things being equal, the resistivity ρ of a nonstoichiometric compound in the ordered state must be lower than in disordered. This is borne out by the available experimental data.

A lower resistivity of ordered compared to a quenched disordered $TiC_{0.625}$ is reported in Ref. [136] for the temperature range 1.5 – 300 K (for example, at 290 K 234×10^{-8} and 208×10^{-8} Ohm m in disordered and ordered $TiC_{0.625}$, respectively). In the 100 – 300 K interval the temperature coefficient of resistivity $d\rho/dT$ of ordered titanium carbide is 1.8 times that of disordered.

Reference [19] reports a jump in the temperature dependence of resistivity of $ZrC_{0.70}$ under conditions of slow warming or slow cooling (at the rate of at most 2 K/min) in the temperature range 1333 – 1353 K (Fig. 11). X-ray analysis showed that the jump is due to the cooling-induced crossover from a high-temperature disordered to a low-temperature ordered state; the resulting ordered phase has the cubic Zr_4C_3-type structure (the conclusion of Ref. [19] about the type of superstructure of ordered zirconium carbide is highly suspect).

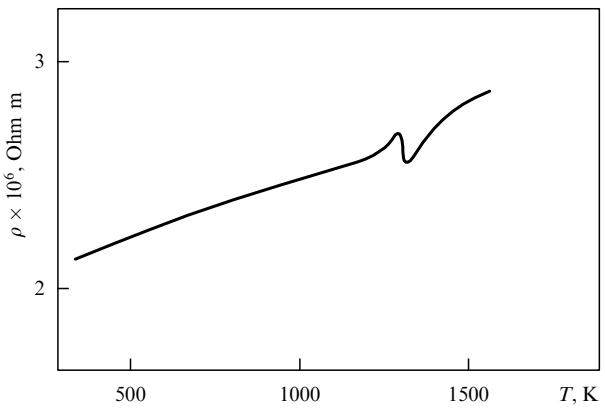

Figure 11. The temperature dependence of the resistivity ρ of nonstoichiometric zirconium carbide $ZrC_{0.70}$ [19].

A 5 – 10 % drop in resistivity at the disorder–order transition $VC_{0.833}$ – V_6C_5, and a corresponding rise in resistivity on disordering in vanadium carbide (Fig. 12) were found in Ref. [137]. The presence of a hysteresis in the $\rho(T)$ dependence indicates that the ordering of vanadium carbide, $VC_{0.833} \rightarrow V_6C_5$, is a first-order phase transition. The behaviour of the resistivity near the $VC_{0.875} \rightleftarrows V_8C_7$ transition temperature (Fig. 13) is analogous to that for

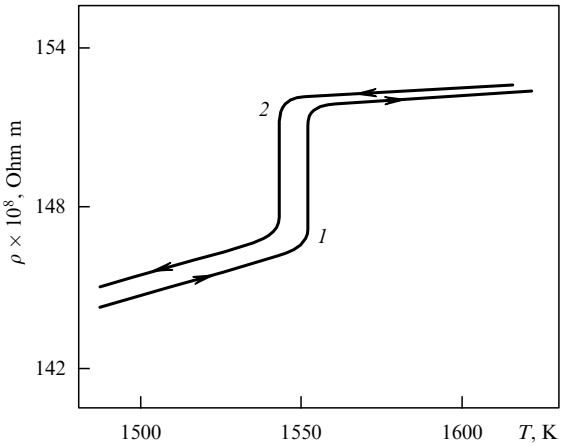

Figure 12. The change in resistivity ρ of ordered V_6C_5 due to heating (*1*) and cooling (*2*) in the neighbourhood of the order–disorder and disorder–order transitions [137].

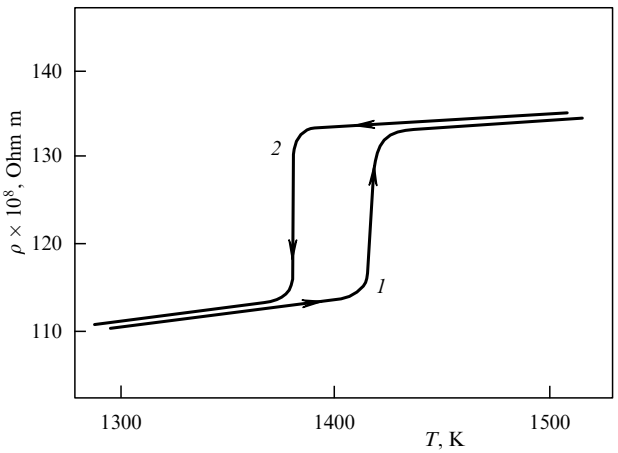

Figure 13. The temperature dependence of the resistivity ρ of ordered carbide V_8C_7 at slow heating (*1*) and slow cooling (*2*) [137].

$VC_{0,833} \rightleftarrows V_6C_5$. As in the case of V_6C_5, the temperature dependence of the resistivity is hysteretic, indicating $VC_{0.875} \rightleftarrows V_8C_7$ to be a first-order phase transition, but the width of the hysteresis is about three times that for $VC_{0.833} \rightleftarrows V_6C_5$ and equals ~ 25 K.

A study of the kinetic properties of vanadium carbide with different vacancy content led the authors of Ref. [137] to the conclusion that the ordered V_8C_7 phase forms even when the composition is close to $VC_{0.833}$. This implies that the ordered V_8C_7 phase has, within its homogeneity region, a lower free energy that the ordered V_6C_5 phase. This assumption is substantiated by heat of transition (ΔH_{trans}) measurements for the corresponding phase transitions [138], which show that the heat released at the $VC_{0.875} \rightarrow V_8C_7$ transition is somewhat greater than that for $VC_{0.833} \rightarrow V_6C_5$ (1.5 ± 0.6 and 1.4 ± 0.7 kJ/mol, respectively).

Figure 14 shows the polythermals of the resistivity of quenched disordered $NbC_{0.83}$ and partially ordered Nb_6C_5 as measured in Ref. [139]. The temperature coefficient of resistivity $d\rho/dT$ of the latter material is much greater than that of the former. At temperatures below the order-disorder transition, the resistivity ρ of partially ordered Nb_6C_5 is lower than in disordered $NbC_{0.83}$. Note that the $\rho(T)$ dependence of

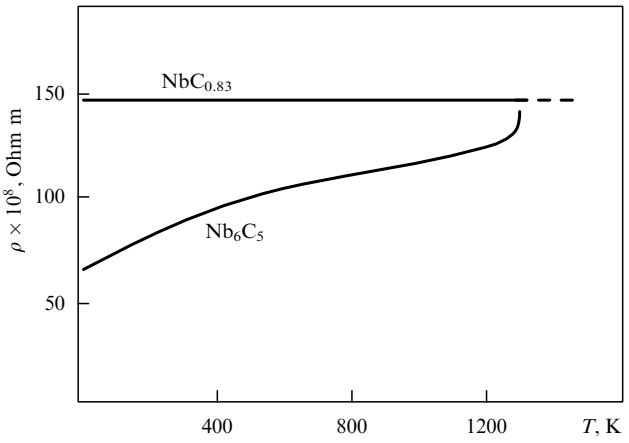

Figure 14. The temperature dependence of the resistivity ρ of disordered carbide $NbC_{0.83}$ and ordered carbide Nb_6C_5 [139].

partially ordered carbide Nb_6C_5 is characteristic of compounds with superconducting transition temperatures around 10 K.

As a whole, the study of nonstoichiometric carbides in various structural states shows that their resistivity is not only highly sensitive to the number but also to the mutual coordination of interstitial atoms and structural vacancies in the crystal lattice.

4.2 Magnetic susceptibility

Magnetic susceptibility is one of the few properties of solids which are determined only by the electronic subsystem and do not depend directly on the phonon energy spectrum.

Although magnetic susceptibility of various nonstoichiometric carbides has been extensively studied, the results are often contradictory. The susceptibility data are usually explained without accounting for the possible ordering of carbon atoms and vacancies.

The effect of ordering on the magnetic susceptibility of a nonstoichiometric compound was first observed in niobium carbide NbC_y [38, 97, 98, 140]. The susceptibility χ was measured in the temperature range 300 – 1300 K using niobium carbide samples in both ordered and disordered state. The structural state of the samples was controlled by neutron diffractometry. A sample was held at each measurement temperature until a time-constant χ was achieved.

The typical temperature dependence $\chi(T)$ for NbC_y in ordered and disordered state is shown in Fig. 15. For the carbide $NbC_{0.83}$ quenched from much above T_{trans} (equilibrium disorder–order transition) and having no superstructure reflections in its neutron diffraction pattern, measurements show a sudden irreversible drop in χ at $T_{\text{trans}}^{\text{noneq}}$, due to the nonequilibrium disordered to equilibrium ordered state transition (Fig. 15). As the temperature is decreased further from $T_{\text{trans}}^{\text{noneq}}$ to T_{trans}, the susceptibility of niobium carbide increases and at T_{trans} experiences a jump as a result of the equilibrium order–disorder transition. The order–disorder transition is reversible, and with lowering temperature the susceptibility decreases as a consequence of the transition from the ordered into a disordered state. On further cooling–warming (annealing–warming) cycling, only the equilibrium order–disorder transition is observed. The temperature behaviour of the susceptibility of samples of other compositions, with a varying degree of disorder, are of the same form

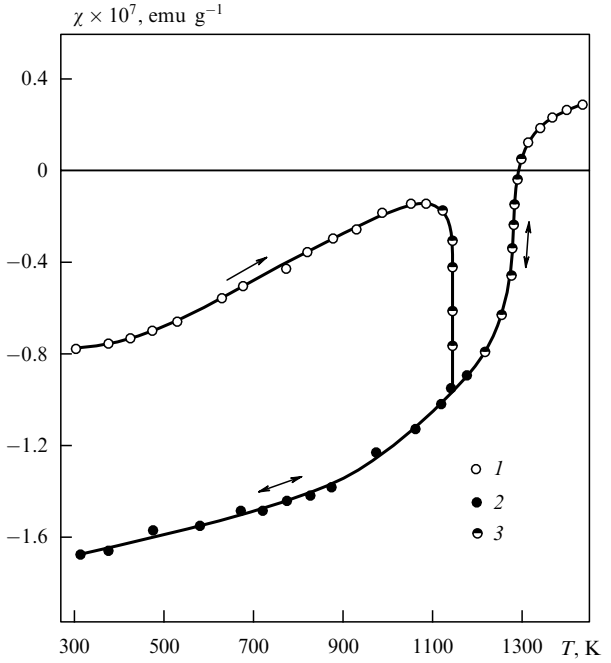

Figure 15. Effect of ordering on the magnetic susceptibility χ of $NbC_{0.83}$: *1*, disordered state; *2*, ordered state; *3*, disorder–order and order–disorder transition regions [140].

as for $NbC_{0.83}$. The neutron diffraction patterns obtained from NbC_y ($0.81 \leqslant y \leqslant 0.88$) samples after a temperature dependence measurement exhibit superstructure reflections indicating that the measurement process brings about ordering and leads to the formation of a M_6C_5-type superstructure.

Magnetic susceptibility measurements showed the $\chi(y)$ minima for NbC_y samples in disordered and ordered state to occur in $NbC_{0.83}$ and $NbC_{0.81}$, respectively (Fig. 16).

A similar study of the susceptibility effect of ordering was made on TaC_y [44 – 46]. For slowly warmed quenched tantalum carbides in the composition range $TaC_{0.82}$ – $TaC_{0.85}$, an earlier unknown effect of irreversible

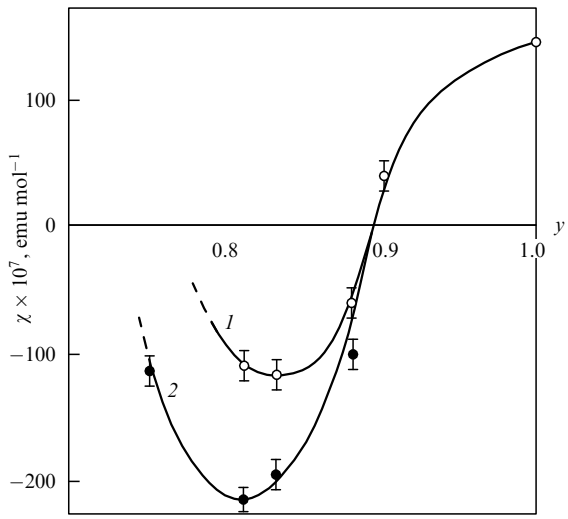

Figure 16. Magnetic susceptibility χ of NbC_y at 300 K in quenched disordered (1) and ordered (2) states [97].

reduction in susceptibility was observed (Fig. 17) at the nonequilibrium transition temperature $T_{\text{trans}}^{\text{noneq}} \approx 960$–1000 K. The temperature of the sudden drop in χ is presumably that for the onset of diffusion of carbon in TaC_y and corresponds to the transition from a quenched nonequilibrium disordered to an equilibrium ordered state. This is confirmed by neutron diffraction data, which imply that the annealing involved in susceptibility measurements to $T < 1100$ K does indeed lead to the appearance, for $TaC_{0.82}$, $TaC_{0.83}$, and $TaC_{0.85}$, of a set of superstructure reflections corresponding to the ordered M_6C_5 phase.

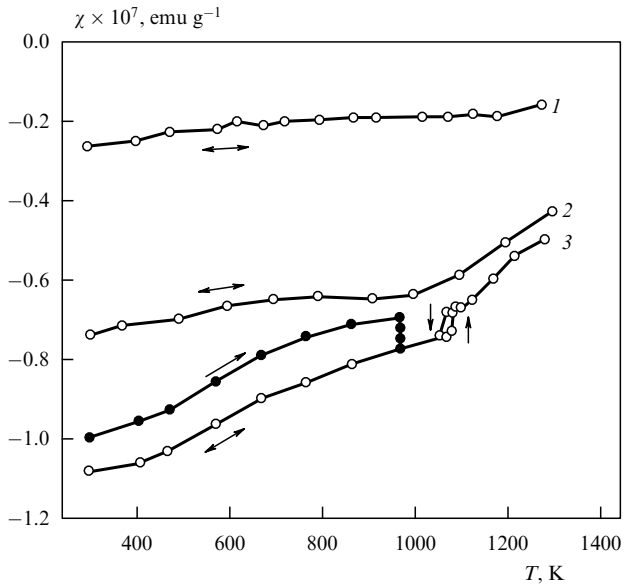

Figure 17. Effect of ordering on the magnetic susceptibility χ of tantalum carbide TaC_y: *1*, $TaC_{0.90}$; *2*, $TaC_{0.76}$; *3*, $TaC_{0.82}$ (arrows indicate the direction of the temperature change; solid circles correspond to quenched nonequilibrium state) [44].

A further rise in temperature led to a smooth growth of T_{trans} followed by a jump at $\chi = 1090$, 1130, and 1150 K for $TaC_{0.82}$, $TaC_{0.83}$ and $TaC_{0.85}$, respectively. The same samples exhibited a temperature hysteresis in susceptibility in the intervals 1070 – 1090, 1100 – 1130, and 1120 – 1150 K for $TaC_{0.82}$, $TaC_{0.83}$, and $TaC_{0.85}$. The reversible susceptibility jump corresponding to the $\chi(T)$ hysteresis region is related to the equilibrium structural order–disorder transition. The occurrence of a hysteresis, i. e., the existence of a two-phase region, shows the order–disorder transition to be a first-order phase transition. As the temperature was lowered further, the susceptibility of the tantalum carbide samples decreased. Note that over the entire temperature range $T < T_{\text{trans}}^{\text{noneq}}$ the susceptibility of a TaC_y ($0.82 \leqslant y \leqslant 0.85$) sample annealed in the measurement process was lower than for the quenched disordered sample of the same composition (Fig. 17). The $\chi(T)$ dependence for TaC_y ($y < 0.80$ and $y \geqslant 0.90$) 0.90 shows no special features (Fig. 17) because these compositions are beyond the region $TaC_{0.79}$ – $TaC_{0.89}$ in which neutron diffraction data show that an ordered phase forms.

Measurements showed that ordering is accompanied by a reduction in susceptibility, the carbide TaC_y exhibiting the greatest susceptibility difference between the disordered and ordered states, $\Delta\chi = = \chi(y, 0) - \chi(y, \eta)$. A similar reduction

has been observed earlier upon the ordering of niobium carbide [38, 97, 98]. Note that in niobium carbide the effect of ordering on χ is much more pronounced than for tantalum carbide of the same carbon content: for example, at 300 K for $NbC_{0.83}$ and $TaC_{0.83}$ the values of χ are 7.6×10^{-6} and 3.9×10^{-6} emu/mol, respectively.

What then can be the explanation for the reduction of magnetic susceptibility in niobium and tantalum carbides upon ordering?

A reduction in susceptibility is possible if the effective mass of a collectivised electron in ordered carbide is greater than that in disordered, i. e., if $m^*_{\text{ord}} < m^*_{\text{disord}}$. If the change in the effective mass of conduction electrons upon ordering is small, then a reduction in χ may be due to the change in the electronic DOS at the Fermi level, $N(E_F)$. However, in niobium carbide $N(E_F)$ is virtually unchanged by ordering [141]. If the same is true for tantalum carbide, our explanation fails.

Another possible answer is a change in the orbital paramagnetic contribution, which depends significantly on the symmetry of the metal atom nearest-neighbour environment. In a disordered nonstoichiometric carbide the symmetry may differ from one metal atom to another, whereas in an ordered M_6C_5 carbide the nearest-neighbour environment of all the metal atoms is identical. Since, on the average, the symmetry of the nearest-neighbour environment in an ordered carbide is higher than in disordered, in the former orbital paramagnetism is weaker than in the latter. Hence follows the observed reduction of susceptibility at the disorder–order transition.

The dependence of the susceptibility on the symmetry of the metal atom nearest-neighbour environment actually implies that the change in χ upon ordering relates to sro formation. A confirmation of the notion that sro affects the magnetic susceptibility of the nonstoichiometric carbides may be found in calculations in Refs [38, 46, 97], in which the experimental data on $\chi(T)$ were used to obtain the sro parameters $\alpha_1(y)$ and $\alpha_2(y)$ in the first and second coordination spheres of the nonmetal sublattice of the ordered NbC_y and TaC_y carbides. In the ordering region $0.81 \leqslant y \leqslant 0.88$ the sro parameters of ordered niobium carbide lie in the intervals $-0.06 > \alpha_1(y) > -0.15$ and $-0.04 > \alpha_2(y) > -0.14$, and of ordered tantalum carbides, in $-0.06 > \alpha_1(y) > -0.08$ and $-0.04 > \alpha_2(y) > -0.09$. The values of α_1 and α_2 for the ordered carbides are negative but do not reach the limiting values ($\alpha_1 = \alpha_2 = -0.20$) characteristic of the perfect superstructure M_6C_5. The deviation of the predicted α_1 and α_2 from their limiting values indicates the lack of complete order in the samples studied.

Thus, calculations confirm that the reduction in the susceptibility of carbides upon ordering is due to the change in the symmetry of the metal atom nearest-neighbour environment, with a resulting decrease in the orbital paramagnetic susceptibility.

The magnetic susceptibility reduction in disordered niobium and tantalum carbides upon the composition change from $MC_{1.00}$ to $MC_{0.83}$ is indicative of the decrease in the electronic DOS at the Fermi level $N(E_F)$.

An attempt to investigate the susceptibility of ordered titanium carbide TiC_y was made in Ref. [142], but the measurement of $\chi(T)$ in this work was carried out on samples outside the homogeneity region of the ordered phase assumed. In addition, there were no measurements on disordered titanium carbide, which does not allow one to deduce from the results of Ref. [142] whether the possible ordering influences the susceptibility of this compound.

4.3 Superconductivity

Practically all nonstoichiometric $B1$-structure interstitial compounds are superconductors with transition temperature T_c of up to 17 K. The superconducting properties of the $B1$ compounds are very sensitive to composition: in a disordered state the highest T_c occurs in vacancy-free stoichiometric $MX_{1.0}$ compounds; as the concentration of vacancies increases, the T_c gets rapidly lower. While the effect of nonstoichiometry on the superconducting properties of $B1$ compounds has attracted quite a detailed study and been repeatedly summarised in the literature [143, 144], virtually no studies exist on the superconductivity-ordering relationship in nonstoichiometric compounds. Only recently have a few studies on the T_c of ordered niobium and tantalum carbides been reported.

The nonstoichiometric $B1$-structure NbC_y has a wide inhomogeneity region extending from $NbC_{1.00}$ to $NbC_{0.70}$. Near-stoichiometric NbC_y ($1.00 > y > 0.98$) has $T_c \sim 11$ K [145, 146]. Already the early studies of the superconducting properties of niobium carbide demonstrated that the T_c decreases rapidly as the concentration of structural vacancies is increased [145, 147, 148]. This work, however, gives no analysis of the arrangement of carbon atoms in the nonmetal sublattice. The change in the niobium carbide structure upon the ordering of carbon atoms and vacancies must lead to a rearrangement of its electronic and phonon spectra as well as to a change in its superconducting properties.

An attempt to elucidate the effect of atomic ordering on the T_c has been made in Ref. [139] using the resistance method to measure the resistivity and superconducting transition temperature of disordered $NbC_{0.83}$ and partially ordered Nb_6C_5 ($NbC_{0.83}$). From that work, disordered $NbC_{0.83}$ has $T_c = 1.7$ K, and for the partially ordered Nb_6C_5 ($NbC_{0.83}$) of the same composition $T_c = 1.1$ K. Since the authors of Ref. [139] failed to obtain a completely ordered Nb_6C_5 crystal, they are not fully justified in concluding that the reduced T_c of the ordered niobium carbide is due to the reduction of the crystal symmetry point group at the disorder–order phase transition.

In contrast to Ref. [139], Ref. [141] shows that ordered Nb_6C_5 ($NbC_{0.83}$) has a higher T_c than the disordered material of the same composition. This is attributed to the presence of translational symmetry in the nonmetal sublattice of the ordered carbide; the lower-T_c disordered niobium carbide exhibits no such symmetry.

A detailed investigation of the effect of ordering on the T_c of niobium carbide was performed in Refs [95, 149], in which an analysis of possible sources of T_c change is also given.

The temperature dependences of the low-temperature heat capacity c_p of the near-stoichiometric carbide $NbC_{0.97}$ and of ordered carbide $NbC_{0.83}$ reveal jumps (Ref. [141], see Fig. 18 of the present work) due to the normal-to-superconducting transition (the calorimetric and inductive T_c values are listed in Table 5). An estimate of the energy gap $\Delta(0)$ using the relation $\Delta(0) = 1.76\, k_B T_c$ yields 1.2 MeV for a near-stoichiometric $NbC_{0.97}$ and 1.1 MeV for disordered $NbC_{0.83}$. This compares well with the tunnel experiment value of $\Delta(0) = 1.6 \pm 0.1$ MeV for $NbC_{0.96}$ [150].

For the remaining niobium carbide samples investigated in Refs [95, 141, 149] (disordered $NbC_{0.845}$ and $NbC_{0.83}$ and partially ordered $NbC_{0.845}$), no superconducting transition was observed down to 4 K.

Table 5. Some characteristics of the electronic structure of nonstoichiometric carbide NbC_y in disordered (*1*) and ordered (*2*) state [95, 149].

Composition	State	γ, mJ g-atom^{-1} K^{-2}	θ_D, K	T_c, K	λ	$N(E_F)$, eV^{-1} atom^{-1}
$NbC_{0.83}$	*1*	1.39 ± 0.01	399 ± 12	2.1	0.48 ± 0.03	0.40 ± 0.03
$NbC_{0.83}$	*2*	1.54 ± 0.01	391 ± 12	8.3	0.69 ± 0.04	0.39 ± 0.03
$NbC_{0.845}$	*1*	1.27 ± 0.01	325 ± 10	2.4	0.52 ± 0.03	0.36 ± 0.03
$NbC_{0.845}$	*2*	1.88 ± 0.02	311 ± 10	< 4.0		
$NbC_{0.97}$	*1*	2.55 ± 0.02	465 ± 14	8.9	0.67 ± 0.04	0.65 ± 0.05

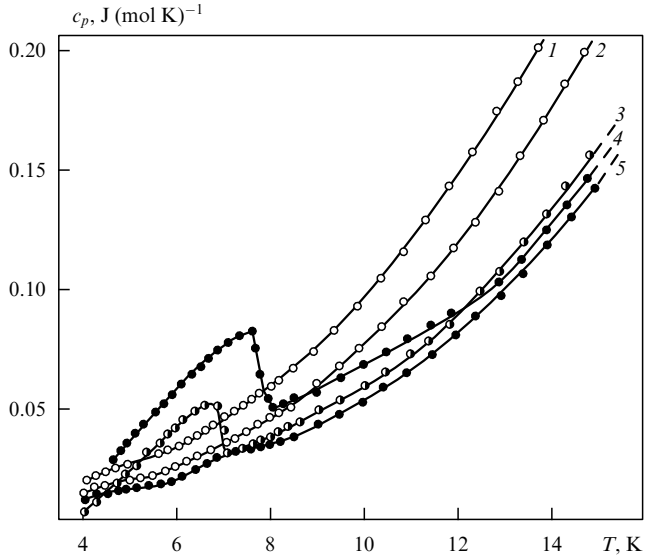

Figure 18. Heat capacity of nonstoichiometric carbide NbC_y at $T < 20$ K: *1*, partially ordered $NbC_{0.845}$; *2*, disordered $NbC_{0.845}$; *3*, ordered $NbC_{0.83}$; *4*, near-stoichiometric disordered $NbC_{0.97}$; *5*, disordered $NbC_{0.83}$ [141].

Of particular note is that the T_c of ordered $NbC_{0.83}$ turns out to be nearly four times that of the disordered carbide of the same composition (8.3 and 2.1 K, respectively). It should also be noted also that the maximum T_c change induced by ordering, 6.2 K, is comparable to the T_c change over the entire homogeneity region of disordered NbC_y (from $T_c < 1$ K for $NbC_{0.70}$ to $T_c = 11.1$ K for $NbC_{1.00}$) and exceeds that for disordered carbide in the composition range $NbC_{0.81}$ – $NbC_{0.88}$ in which the ordered Nb_6C_5 phase forms (for $NbC_{0.81}$ and $NbC_{0.88}$ T_c is 1.5 and 4.4 K, respectively, giving $\Delta T_c \approx 2.9$ K).

In the analysis of the superconducting properties of *B*1 carbides, it is customary to employ strong-coupling approximation accounting for the electron-phonon interaction. This is actually tantamount to renormalizing the electronic DOS at the Fermi level, $N(E_F)$, via the use of the electron-phonon coupling constant λ.

Approximating the heat capacity data for nonstoichiometric niobium carbide at $T_c < T < 20$ K by

$$c(y, T) = (1 + y)(\gamma T + \beta T^3) \tag{14}$$

enabled the coefficient of electronic heat capacity $\gamma = (\pi^2 k_B^2 N_A/3)(1 + \lambda) N(E_F)$ and the Debye temperature $\theta_D = (6\pi^4 k_B N_A/5\beta)^{1/3}$ to be determined for all NbC_y samples studied [95, 149] (Table 5).

The significant difference in magnetic susceptibility χ (97, 98, 140) and superconducting transition temperature between disordered and ordered niobium carbide [95, 141, 149] is indicative of order-induced changes in the electronic and phonon spectra. The data obtained enable one to determine certain characteristics of the electronic structure and to find out their change upon ordering.

In discussing the phonon mechanism of superconductivity in niobium carbide, it is convenient to use the semi-empirical McMillan's formula [151]

$$T_c = \frac{\theta}{1.45} \exp\left[-\frac{1.04(1 + \lambda)}{\lambda - \mu^* (1 + 0.62\lambda)}\right]. \tag{15}$$

The numerical values of the coefficients in Eqn (15) were obtained by McMillan by analysing the shape of the Nb phonon spectrum. The pseudopotential μ^* for electronic Coulomb repulsion can be determined from the isotope effect, by measuring the T_c and the isotope shift δT_c. For the transition metals, μ^* is not large and has a value of 0.10 – 0.15. The strong-coupled formula (15) and the availability of data on T_c and θ_D (Table 5) have enabled the electron-phonon coupling constant λ to be evaluated. The calculation of Ref. [95] assumed the NbC_y Coulomb pseudopotential to be $\mu^* = 0.13$ [139, 148].

The electronic DOS at the Fermi level $N(E_F)$ was calculated, using the obtained values of γ and λ, from

$$N(E_F) = \frac{3\gamma}{\pi^2 k_B^2 N_A (1 + \lambda)}. \tag{16}$$

The results on λ and $N(E_F)$ are presented in Table 5.

The data in Table 5 show that in disordered niobium carbide a decrease in carbon content (increase in vacancy concentration) leads to a decrease in the electronic DOS $N(E_F)$. Analogous results were obtained in Refs [147, 148]. This behaviour of $N(E_F)$ as a function of the composition of NbC_y is in good agreement with magnetic susceptibility data (see Section 4.2), which show that as the composition of disordered carbide is varied from $NbC_{1.00}$ to $NbC_{0.83}$, the Fermi DOS decreases. Hall coefficient measurements in turn show that a decrease in carbon content in niobium carbide increases the concentration of conduction electrons [152].

The conduction band in group-V transition metal carbides is less than half filled. A decrease in the electronic DOS at the Fermi level $N(E_F)$ and an increase in the number of conduction electrons due to vacancy formation can occur simultaneously if a local DOS peak appears in the conduction band below the Fermi energy. In fact, a SCF-X_α cluster calculation of the electronic structure of nonstoichiometric niobium carbide showed [93] that the formation of a carbon vacancy leads to a narrow peak in the spectrum of filled states. The peak is 2 eV below E_F. At a sufficiently high carbon vacancy content the NbC_y spectrum exhibits a vacancy band below NbC_y mainly filled by Nb4*d* electrons [153]. Thus, a decrease in the carbon content in niobium carbide leads to a decrease in the electronic DOS $N(E_F)$ and to a change in the fine structure of the energy spectrum below the Fermi level.

According to Refs [95, 149] (Table 5), the behaviour of the T_c in the ordering process is dominated by the change in the electron-phonon coupling. The marked change (a factor of 1.5) in the electron-phonon interaction constant upon ordering is presumably due to the fact that translational symmetry does not exist in disordered niobium carbide but does in ordered. The low T_c for partially ordered $NbC_{0.845}$ can then be attributed to the deviation of the carbide from the stoichiometry of the Nb_6C_5 ordered phase and hence, to the lack of complete order in the atom and vacancy arrangement.

For a near-stoichiometric carbide $NbC_{0.97}$, the value of T_c is somewhat larger than for ordered $NbC_{0.83}$; this is presumably due to the electronic DOS $N(E_F)$ being greater in $NbC_{0.97}$. The electron-phonon coupling in ordered $NbC_{0.83}$ and in $NbC_{0.97}$ is essentially the same (Table 5).

In $B1$ and $A15$ superconductors the electron-electron interaction takes place by exchange of phonons. References [95, 149] assumed the phonon mechanism of superconductivity and employed the strong-coupling approximation to determine λ and $N(E_F)$. The calculation used volume-averaged crystal properties, however. For a disordered nonstoichiometric carbide with isotropic crystal structure this is quite justifiable. However, for a disordered nonstoichiometric carbide this estimate of $N(E_F)$ characterises the average of the electronic DOS over the entire volume of the anisotropic crystal, whereas the true density distribution $N(E_F)$, depending as it does on the particular manner in which the atoms are distributed in the lattice of the ordered compound, may be inhomogeneous in the crystal volume and may have maxima and minima in its spatial pattern.

The ordered Nb_6C_5 ($NbC_{0.83}$) has a peculiar layered crystal structure [10, 38 – 42]. Accordingly, in order to explain the superconducting properties of ordered and disordered niobium carbide, a two-dimensional model of superconductivity has been proposed [95, 149, 154]. An outline of the model is as follows.

Let us consider in detail the crystal structure of the stoichiometric $NbC_{1.00}$. In the $[111]_{B1}$ direction, the structure may be thought of as alternating close-packed $(111)_{B1}$ planes consisting of either metal or nonmetal atoms (Fig. 19a).

As disordered niobium carbide deviates from stoichiometry, some of nonmetal lattice sites become vacant, with the result that the crystal structure is locally distorted, and instead of complete nonmetal planes of carbon atoms alone, defect nonmetal planes, with both carbon atoms and vacancies, appear (Fig. 19b). In disordered NbC_y vacancies arrange themselves statistically, so that local atom displacements are directed at random, and the atomic planes are practically all distorted.

The disorder–order phase transition in niobium carbide leads to a fundamentally different arrangement of carbon atoms and vacancies. Formation of the monoclinic (space group $C2/m$) Nb_6C_5 ordered phase is related to three wave vector stars $\{\mathbf{k}_9\}$, $\{\mathbf{k}_4\}$, and $\{\mathbf{k}_3\}$ (Table 2) and is described by three lro parameters η_9, η_4, and η_3 [63, 64]. If only the nonmetal sublattice is considered, then the structure of completely ordered niobium carbide consists of complete and defective ordered nonmetal planes alternating in the $[111]_{B1}$ direction (Fig. 19c); the parameter η_9 being responsible for the preservation of the order of alternation and for the rearrangement of carbon atoms and vacancies between the planes. The η_4 and η_3 parameters are only responsible for the mutual arrangement of atoms and vacancies in nonmetal planes and do not affect the relative content of carbon atoms and vacancies in the planes [63].

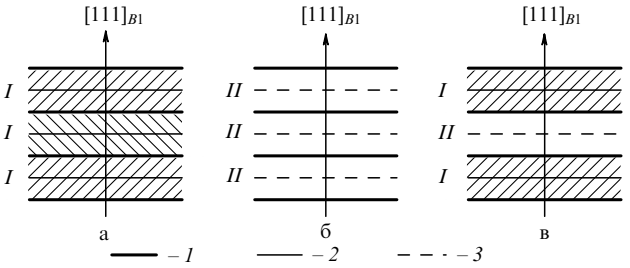

Figure 19. Mutual arrangement of the $(111)_{B1}$ atomic planes in stoichiometric carbide $NbC_{1.00}$ (a), nonstoichiometric disordered NbC_y (b), and fully ordered Nb_6C_5 ($NbC_{0.83}$) (c): *1*, Nb atom plane; *2* and *3*, complete and defective nonmetal atomic planes; *I* and *II*, quasi-2D complete and defective layers [95, 149].

The quasi-2D model of Ref. [95] assumes that superconductivity in niobium carbide is due to the presence of type-*I* layers (Fig. 19) consisting of two neighbouring metal planes with a complete nonmetal plane in-between. It is also assumed that the appearance of vacancies in nonmetal planes degrades the superconducting properties of the quasi-2D layers. Let us see how the T_c of niobium carbide will change in this model. For a disordered state, the highest electronic DOS $N(E_F)$ occurs in stoichiometric $NbC_{1.00}$, in which only quasi-2D type-*I* layers are present (Fig. 19a); an increase in vacancy concentration in disordered carbide is accompanied by a monotonic decrease in $N(E_F)$ (Table 5) and by the appearance of defect quasi-2D type-$N(E_F)$ layers (Fig. 19b). Then clearly in the complete quasi-2D type-*I* layers the DOS is much higher than in defective quasi-2D type-*II* layers. For this reason, a deviation of the carbon atom concentration from stoichiometry should result in a rapid reduction in T_c, which is in line with the results obtained in Refs [95, 141, 145, 147 – 149].

As seen in Fig. 19c, ordered niobium carbide contains complete superconducting type-*I* layers similar to those in the defect-free stoichiometric carbide. Note that the formation of complete nonmetal planes in NbC_y in the composition range $(5/6 \leqslant y \leqslant 1)$ requires that lro (η_9) be as high as possible, and for $y < 5/6$ this process is unlikely even then because of the high vacancy concentration. The appearance in nonstoichiometric niobium carbide of superconducting type-*I* layers with their highest possible $N(E_F)$ must raise the T_c to about values for stoichiometric $NbC_{1.0}$, as indeed observed [95, 149].

Thus, in nonstoichiometric niobium carbide a quasi-2D layered structure appears upon ordering. For ordered quasi-2D Nb_6C_5 ($NbC_{0.83}$) $T_c = 8.3$ K, i. e., about four times higher than $T_c = 2.1$ K in disordered $NbC_{0.83}$. Presumably, the rise in T_c at the formation of a quasi-2D structure is due to the presence of periodic local $N(E_F)$ maxima which correspond to complete, well superconducting, quasi-2D type-*I* layers [95].

The 2D conduction electron distribution model suggests that the superconducting transition temperature of $NbC_{0.97}$, with low content of structural vacancies, should be close to that of ordered $NbC_{0.83}$. Experimentally [95, 141], the T_c of ordered niobium carbide is somewhat lower. There are two possible reasons for this. First, in ordered $NbC_{0.83}$ the degree of lro is somewhat less than the maximum degree. In this case

some of the complete nonmetal planes become defective, and the complete superconducting layers reduce in number. Second, even for the maximum degree of lro in $NbC_{0.83}$, all the superconducting type-*I* layers are in the neighbourhood of defective nonmetal planes (Fig. 19c). The same kind of argument is given in Refs [155, 156], which present experimental and theoretical studies of the Nb bicrystal twinning plane: a unique example of a two-dimensional physical system. It is shown that a normal metal surrounding the twinning plane degrades the superconductivity of the two-dimensional layer significantly.

A rise in the T_c of nonstoichiometric niobium carbide due to annealing of the $NbC_{0.87}$ single crystal is found in Ref. [157]. On quenching to 1600 K, disordered $NbC_{0.87}$ had $T_c \approx 4$ K, and on annealing at $T = 1200$–1400 K, as a result of ordering, the T_c reaches a value of 8.6 K. These results are accounted for completely by the quasi-2D superconductivity model of Refs [95, 149].

The effect of ordering on the T_c of tantalum carbide was examined in Ref. [49]. Measurements showed that the T_c of disordered TaC_y decreases rapidly from 10.2 K for $TaC_{1.00}$ to 1.5 K for $TaC_{0.83}$ as the carbon content is decreased. The T_c data on disordered TaC_y are in good agreement with those of Refs. [145, 147]. The T_c values of the ordered carbides $TaC_{0.87}$ and $TaC_{0.83}$ turned out to be slightly (by 0.3 and 0.6 K, respectively) higher than in disordered carbides of the same composition. The observed effect of ordering was not large, so one can only speak of an incipient tendency of nonstoichiometric tantalum carbide toward higher T_c as a result of ordering. This distinguishes tantalum carbide from niobium carbide, for which the T_c increased several-fold upon ordering. That the effect of ordering on the T_c is different in these two carbides is presumably due to the difference in the nature of superstructures that form in them.

In fact, the ordering of niobium carbide leads to the formation of an M_6X_5 type superstructure, with quasi-2D type-*I* and -*II* layers alternating along $[111]_{B1}$ (Fig. 19). The presence of complete quasi-2D I layers in the ordered carbide resulted in a higher T_c compared to disordered material, in which no such layers exist.

As regards TaC_y, this gives rise to an incommensurate superstructure [47 – 49] in which even at the maximum lro, superconducting quasi-2D type-*I* layers are 8 – 9 times as rare as in the commensurate M_6X_5 superstructure. However, in the tantalum carbide studied, basic lattice parameter [74] and heat capacity [65, 66] data show that the maximum degree of order was not attained, and the percentage of superconductivity-producing complete quasi-2D layers in ordered carbide was by far lower than in the ideal commensurate M_6X_5 superstructure. Hence the small transition temperature difference between $TaC_{0.83}$ with a noncommensurate superstructure and the disordered carbide of the same composition.

If, in the homogeneity region of the ordered phase of tantalum carbide ($TaC_{0.79}$ – $TaC_{0.89}$), one succeeds in obtaining a commensurate M_6X_5 type superstructure with a degree of order close to the maximal, it might be expected that the effect of ordering on the T_c will be relatively large and comparable to the T_c change observed at the ordering of niobium carbide.

4.4 Heat capacity

To date, the effect of ordering on heat capacity has been studied, to a greater or lesser degree, for titanium, niobium, and tantalum carbides.

We shall first discuss the effect of ordering on heat capacity at temperatures below 30 K.

The low-temperature heat capacity of disordered and ordered NbC_y was investigated in Refs [141, 149]. The temperature dependence of the heat capacity of NbC_y in various structural states at $T < 20$ K is shown in Fig. 18. In the temperature range studied, ordered $NbC_{0.83}$ and $NbC_{0.845}$ have a higher heat capacity than disordered carbides of the same composition.

The effect of ordering on the heat capacity of $TiC_{0.625}$ at $T < 5$ K was examined in Ref. [136]. Measurements showed that the heat capacity of ordered rhombohedral carbide is about 3% less than that of disordered $TiC_{0.625}$. The heat capacity difference $\Delta c\,(T) = c\,(y, \eta, T) - c\,(y, 0, T)$ was described by $\Delta c\,(T) = \Delta\gamma T + \Delta\beta T^3$, where $\Delta\gamma = -(0.18 \pm 0.03) \times 10^{-3}$ J mol^{-1}K^{-2} and $\Delta\beta = -(0.6 \pm 1.7) \times 10^{-6}$ J mol^{-1}K^{-2}.

The most extensive studies of the effect of structural state on the heat capacity of niobium and tantalum carbides were made in the temperature range 70 – 300 K [65, 66, 158, 159].

The polythermals of the heat capacity of MC_y for $70 < T < 300$ K were described with the use of the superposition model [160] accounting for the contributions to the heat capacity from the acoustic and optical phonons:

$$c_p\,(y, T) = \frac{1+y}{2}\left[c_D\left(\frac{\theta_D}{T}\right) + c_E\left(\frac{\theta_E}{T}\right)\right], \qquad (17)$$

where c_D and c_E are the Debye and Einstein heat capacity functions, and θ_D and θ_E are the Debye and Einstein characteristic temperatures. Table 6 lists θ_D and θ_E values for all the niobium and tantalum carbides studied in Refs [65, 158, 159].

Fig. 20 and 21 show the composition dependences of heat capacity for niobium and tantalum carbides in disordered and ordered state. As seen in the figures, the heat capacity of the ordered carbides exceeds that of the same carbides in disordered state. The maximum value of the heat capacity difference $\Delta c_p(300) = c_p^{\rm ord}(300) - c_p^{\rm disord}(300)$ occurs in $NbC_{0.83}$ and $TaC_{0.83}$, which correspond to the stoichiometric composition of ordered M_6C_5-type phase.

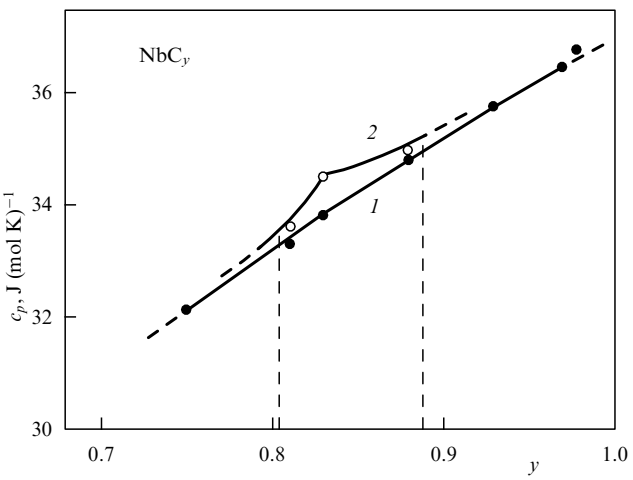

Figure 20. Heat capacity of niobium carbide NbC_y in disordered (*1*) and equilibrium ordered (*2*) state at 300 K (points give the experimental values; solid line is for the approximation $\eta = \eta_{\rm trans}$). The dash-dot line shows the boundary of the homogeneity region of the Nb_6C_5 ordered phase [158, 159].

Table 6. Debye temperature θ_D, Einstein temperature θ_E, and heat capacity c_p, of niobium carbide NbC_y and tantalum carbide TaC_y in disordered (1) and ordered (2) state at 300 K [66, 159].

Composition	State	θ_D, K	θ_E, K	$c_p(300)$, J (mol K)$^{-1}$	$\Delta c_p\,(y,\eta,300)$, J (mol K)$^{-1}$		
					experiment	calculation	
						$\eta\,(300) = \eta_{trans}$	$\eta\,(300) = \eta_{max}$
$NbC_{0.75}$	*1*	347	844	32.15			
$NbC_{0.81}$	*1*	375	825	33.35	0.50	0.55	1.31
$NbC_{0.81}$	*2*	365	801	33.85			
$NbC_{0.83}$	*1*	358	823	33.89	0.60	0.56	1.39
$NbC_{0.83}$	*2*	359	789	34.49			
$NbC_{0.88}$	*1*	355	825	34.81	0.03	0.40	0.72
$NbC_{0.88}$	*2*	352	825	34.84			
$NbC_{0.93}$	*1*	375	813	35.78			
$NbC_{0.97}$	*1*	366	820	36.48			
$NbC_{0.98}$	*1*	377	827	36.81			
$TaC_{0.81}$	*1*	256	848	33.84	0.14	0.38	0.90
$TaC_{0.81}$	*2*	252	840	33.98			
$TaC_{0.84}$	*1*	258	818	34.91	0.60	0.38	0.88
$TaC_{0.84}$	*2*	243	788	35.51			
$TaC_{0.88}$	*1*	261	809	35.81	0.11	0.28	0.50
$TaC_{0.88}$	*2*	259	803	35.92			
$TaC_{0.93}$	*1*	256	824	36.52			
$TaC_{0.96}$	*1*	252	848	36.66			
$TaC_{1.00}$	*1*	263	875	36.85			

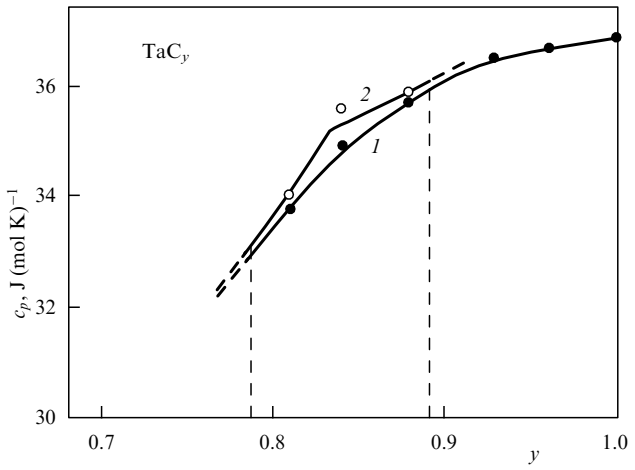

Figure 21. Heat capacity of tantalum carbide TaC_y in disordered (*1*) and equilibrium ordered (*2*) state at 300 K (points show the experimental values; solid line is calculated using the approximation $\eta = \eta_{trans}$). The dash-dot line shows the boundary of the homogeneity range of the ordered phase Ta_6C_5 [65, 66].

In Ref. [66], certain aspects of the order parameter functional (OPF) method [8, 10, 56] were used to explain the influence of ordering on the heat capacity of nonstoichiometric, interstitial *B*1 (NaCl) MX_y compounds. Whereas the physical basis for the OPF is the mean field approximation, it belongs to the family of cluster methods as far as its formalism is concerned. The description of ordering in Ref. [66] involves a basic cluster in the form of an octahedron of six sites of the fcc nonmetal lattice, which constitute the nearest-neighbour environment of the metal atom located at the centre of the figure. According to Ref. [66], in the OPF method the heat capacity of nonstoichiometric MC_y in disordered ($\eta = 0$) and ordered ($\eta \neq 0$) states can be represented as a function of composition y, lro parameter η, and temperature T as follows:

$$c_p\,(y,0,T) = \frac{\partial H_0^*(T)}{\partial T} + y\,\frac{\partial H_1^*(T)}{\partial T} + y^2\,\frac{\partial H_2^*(T)}{\partial T}\,, \qquad (18)$$

$$c_p\,(y,\eta,T) = \frac{\partial H_0^*(T)}{\partial T} + y\,\frac{\partial H_1^*(T)}{\partial T} + P_0^{(2)}\,\frac{\partial H_2^*(T)}{\partial T} + H_2^*(T)\,\frac{\partial P_0^{(2)}}{\partial T}\,, \qquad (19)$$

where $P_0^{(2)}$ is the probability of occurrence, within the basic cluster, of a complete C–C pair in the nonmetal sublattice of the MC_y being ordered; H_0^*, H_1^* and H_2^* are the coefficients of the power-series expansion in y of the enthalpy of disordered MC_y. Analysis of thermodynamic data suggests that for disordered carbides this expansion need be kept to the second order only [8, 10, 143]:

$$(H_T - H_{298})^{\text{disord}}_{MC_y} = H_0^*(T) + yH_1^*(T) + y^2H_2^*(T)\,. \qquad (20)$$

When undergoing ordering, niobium and tantalum carbides give rise to M_6C_5-type superstructure [52], for which the probability $P_0^{(2)} = y^2 - \eta^2/36$ under equilibrium conditions [8, 10]. In view of this and Eqns (18) and (19), the heat capacity difference $\Delta c_p\,(y,\eta,T) = c_p\,(y,\eta,T) - c_p\,(y,0,T)$ of nonstoichiometric MC_y in ordered and disordered states is

$$\Delta c_p\,(y,\eta,T) = -\frac{\eta^2}{36}\,\frac{\partial H_2^*(T)}{\partial T} - \frac{\eta}{18}\,\frac{H_2^*(T)\,\partial\eta}{\partial T}\,. \qquad (21)$$

Let us discuss Eqn (21) in more detail. According to Refs [8, 10, 56], a necessary condition for ordering in substitution solid solutions and nonstoichiometric compounds, with a substitution solution formed by substitutional atoms and vacancies, is the nonlinear dependence of the enthalpy of formation and free energy on the composition of disordered

compound. If the enthalpy of a disordered compound MX_y is quadratic in y, then its OPF free energy is described by

$$F(y,0,T) = F_0(T) + yF_1(T) + y^2F_2(T) - TS_c(y,0)\,, \quad (22)$$

where $F_0(T)$, $F_1(T)$, and $F_2(T)$ are energy parameters, and $S_c(y,0)$ is the configurational entropy of the disordered compound. Given this dependence of the free energy of disordered compound on y and T, a necessary condition for ordering is $F_2(T) > 0$ [56]; in particular, ordering is possible if the parameter F_2 is a temperature-independent positive constant, i.e., $F_2 = \text{const} > 0$. This is the case if in Eqn (20) the coefficient $H_2^*(T) \equiv 0$ and hence $\partial H_2^*(T)/\partial T \equiv 0$, i. e., if the enthalpy and free energy of disordered compound MX_y are linear functions of its composition y. Thus, the heat capacities of a nonstoichiometric compound in ordered and disordered states may be equal ($\Delta c_p \equiv 0$) when $F_2 = \text{const} > 0$.

Most generally, $H_2^*(T) \neq 0$ and $\partial H_2^*(T)/\partial T \neq 0$. Below T_{trans} the derivative $\partial\eta/\partial T$ is negative, since as the temperature is lowered the degree of order increases. But then Eqn (21) implies that the sign of Δc_p is determined by the values of $H_2^*(T)$ and $\partial H_2^*(T)/\partial T$. The derivative $\partial H_2^*(T)/\partial T$ is the coefficient of the quadratic term in the series expansion (18) of the heat capacity of disordered compound MX_y.

Let $c_p(y,0,T)$ be a convex function of y, then $\partial H_2^*(T)/\partial T < 0$ and $H_2^*(T) < 0$, rendering the first term in Eqn (24) positive, and the second negative. With increasing temperature the former decreases and the latter increases in absolute value, so that the difference Δc_p is also temperature dependent. At 300 K $\partial\eta/\partial T$ nearly vanishes, the difference $\Delta c_p > 0$, and the heat capacity of a nonstoichiometric compound in ordered state exceeds that in disordered one. With increasing temperature the value of Δc_p decreases and may become negative.

If $c_p(y,0,T)$ is a negative function of y, then $\partial H_2^*(T)/\partial T > 0$ and $H_2^*(T) > 0$; in this case a similar argument shows that at $T = 300$ K the difference $\Delta c_p < 0$, but with increasing temperature it increases and may become positive as T_{trans} is approached.

For disordered NbC_y and TaC_y, the $c_p(y)$ dependences are positive functions of y (Figs 20, 21), so according to Ref. [66], at $T = 300$ K the heat capacity of the ordered carbides must be greater than for quenched disordered carbides of the same composition, i. e., $\Delta c_p(300) > 0$. The experimental results of Refs [65, 159] shown in Table 6 support this conclusion.

A comparison of the experimental and theoretically predicted values of $\Delta c_p(300)$ allowed estimation [8, 52, 66] of the degree of lro in the ordered niobium and tantalum carbides investigated. The value of $\Delta c_p(300)$ was calculated in two ways.

One approach assumed that at 300 K the carbide sample studied reach the maximum possible degree of lro, i. e., $\eta(300) = \eta_{\max}$; then the derivative $\partial\eta/\partial T = 0$, since the order parameter $\eta(300)$ is a constant quantity. Within the homogeneity region of the ordered M_6C_5 phase that forms in NbC_y and TaC_y, the value of $\eta_{\max}(y)$ is determined from Eqn (6).

The second approach to the calculation of $\Delta c_p(300)$ assumed that, because of the low diffusion mobility of atoms at 300 K, the lro parameter in ordered carbide samples remains, in absolute value, the same as at the disorder–order transition temperature, i. e., $\eta(300) = \eta_{\text{trans}}$ (η_{trans} values are taken from Ref. [8]). Clearly, $\partial\eta/\partial T = 0$ in this approximation also.

A comparison of the experimental and computed values of $\Delta c_p(300)$ (Table 6) shows that the values obtained in the approximation $\eta(300) = \eta_{\text{trans}}$ come closest to experiment.

5. Conclusions

Recent studies have added considerable insight into the atomic and vacancy ordering in nonstoichiometric carbides. While earlier work has focused on structural and crystallographic aspects of ordering in these compounds [11, 12, 18, 81, 143, 161], at present the effects of ordering on carbide properties are the top priority. There is much evidence to show that ordering effects are of comparable magnitude to property changes occurring in the homogeneity region of a disordered carbide. This allows a modification and subtle special-purpose tailoring of the properties of nonstoichiometric carbides by creating short-range and long-range order without changing composition. Further study of the properties and structure of highly nonstoichiometric compounds in states of varying (from $\eta = 0$ to $\eta = \eta_{\max}$) degree of order is necessary, and this not only for carbides but also for cubic $B1$-structure nitrides and oxides of the transition metals. The collection and evaluation of such data will contribute to the development of the theory of disorder–order structural phase transitions in highly nonstoichiometric compounds.

The author would like to thank A I Gusev for much help and encouragement in preparing the manuscript and the Russian Foundation for Basic Research (RFBR) for financial support (project No 95-02-03549-a).

References

1. Hagg G *Ztschr. Phys. Chem.* **12** (1) 33 (1931)
2. *Soedineniya Peremennogo Sostava* (Variable Composition Compounds and their Solid Solutions) (Ed. B F Ormont) (Leningrad: Khimiya, 1969)
3. Goldschmidt H J *Splavy Vnedreniya* (Interstitial Alloys) (Moscow: Mir, 1971)
4. Andrievskiĭ R A, Umanskiĭ Ya S *Fazy Vnedreniya* (Interstitial Phases) (Moscow: Nauka, 1977)
5. Shveikin G P et al. *Soedineniya Peremennogo Sostava i ikh Tverdye Rastvory* (Variable Composition Compounds and their Solid Solutions) (Sverdlovsk: Ural'skiĭ Nauchnyi Tsentr Akad. Nauk SSSR, 1984)
6. Gusev A I et al. *Usp. Khimii* **55** 2067 (1986) [*Russ. Chem. Reviews* **55** 1175 (1986)]
7. Gusev A I, Rempel' A A *Termodinamika Strukturnykh Vakansii v Nestekhiometricheskikh Fazakh Vnedreniya* (Thermodynamics of Structural Vacancies in Nonstoicheiometric Interstitional Phases) (Sverdlovsk: Ural'skiĭ Nauchnyi Tsentr Akad. Nauk SSSR, 1987)
8. Gusev A I *Fizicheskaya Khimiya Nestekhiometricheskikh Tugoplavkikh Soedinenii* (Physical Chemistry of Nonstoicheiometric High-Melting Compounds) (Moscow: Nauka, 1991)
9. Rempel A A, Gusev A I, in *Advanced Solid State Chemistry* (Materials Science monographs. Vol. 60) / Eds M Frumar, V Cerný, L Tichý (Amsterdam: Elsevier, 1989) p. 14
10. Gusev A I, Rempel' A A *Strukturnye Fazovye Perekhody v Nestekhiometricheskikh Soedineniyakh* (Structural Phase Transitions in Nonstoicheiometric Compounds) (Moscow: Nauka, 1988)
11. Gusev A I *Phys. Stat. Sol. B* **163** (1) 17 (1991)
12. Gusev A I, Rempel A A *Phys. Stat. Sol. A* **135** (1) 15 (1993)
13. Goretzki H *Phys. Stat. Sol.* **20** (2) K141 (1967)
14. Karimov I et al. *Izv. Akad. Nauk Uzb. SSR Ser. Fiz.-Tekh. Mat. Nauk* **4** 81 (1979)
15. Khaenko B V, Kukol' V V *Kristallografiya* **34** 1513 (1989) [*Sov. Phys. Crystallogr.* **34** 965 (1989)]

16. de Novion C H *The Physics and Chemistry of Carbides, Nitrides and Borides* / Ed. R Freer (Netherlands: Kluwer Academic Publishers, 1990) p. 329
17. Gusev A I, Rempel' A A *Dokl. Akad. Nauk* (Russia) **332** 717 (1993) [*Phys. Dokl.* **332** 717 (1993)]
18. Khaenko B V *Izv. Akad. Nauk SSSR, Neorg. Mater.* **15** 1952 (1979) [*Inorg. Mater. (USSR)*]
19. Obata N, Nakazawa N *J. Nucl. Mater.* **60** (1) 39 (1976)
20. Gusev A I *Dok. Akad. Nauk SSSR* **313** 887 (1990) [*Sov. Phys. Dokl.* **35** 615 (1990)]
21. Gusev A I *Fiz. Tverd. Tela* (Leningrad) **32** 2752 (1990) [*Sov. Phys. Solid State* **32** 1595 (1990)]
22. Gusev A I, Rempel' A A *Zh. Fiz. Khim.* **65** 625 (1991) [*Russ. J. Phys. Chem.* **65** 330 (1991)]
23. Gusev A I, Rempel A A *J. Phys. Chem. Solids.* **55** 299 (1994)
24. Gusev A I, Rempel A A *Proc. Intern. Conf. on Advances in Hard Materials Production* (Bonn, 1992) p. 39
25. Gusev A I *Dokl. Akad. Nauk* (*SSSR*) **322** 918 (1992) [*Sov. Phys. Dokl.* **37** 84 (1992)
26. Khaenko B V *Poroshk. Metall.* **17** 71 (1978) [*Sov. Powder Metall. Met. Ceram* **17** 55 (1978)]
27. Venables J D, Kahn D, Lye R G *Philos. Mag.* **18** (151) 177 (1968)
28. Billingham J, Bell P S, Lewis M H *Acta Crystallogr. A* **28** (6) 602 (1972)
29. Billingham J, Bell P S, Lewis M H *Philos. Mag.* **25** (3) 661 (1972)
30. Khaenko B V, Fak V G *Izv. Akad. Nauk SSSR, Neorg. Mater.* **14** 1294 (1978) [*Inorg. Mater.* (USSR) **14** 1011 (1978)]
31. de Novion C H, Lorenzelli R, Costa P *Compt. Rend. Acad. Sci. B* **263** (13) 775 (1966)
32. Alyamovskiĭ S I et al. *Zh. Neorg. Khim.* **2** 1738 (1968) [*Russ. J. Inorganic Chem.* **13** 895 (1968)]
33. Arbuzov M P et al. *Ukr. Fiz. Zh.* (Russ. Ed.) **22** 291 (1977)
34. Rudy E, Brukl C E *J. Amer. Ceram. Soc.* **50** (5) 265 (1967)
35. Lewis M H, Billingham J, Bell P S *Proc. of 5th Intern. Mater. Symp.* (Berkeley, California, 1972) p. 1084
36. Landesman J P et al. *J. Phys. C: Solid State Phys.* **18** (4) 809 (1985)
37. Christensen A N *Acta Chem. Scand. A* **39** (10) 803 (1985)
38. Rempel' A A , Gusev A I *Uporyadochenie v Nestekhiometricheskom Monocarbide Niobiya* (Ordering in Nonstoichiometric Niobium Monocarbide) (Sverdlovsk: Ural'skiĭ Nauchnyi Tsentr Akad. Nauk SSSR, 1983)
39. Rempel' A A et al. *Dokl. Akad. Nauk SSSR* **275** 883 (1984) [*Sov. Phys. Dokl.* **29** 257 (1984)]
40. Gusev A I, Rempel' A A *Fiz. Tverd. Tela* (Leningrad) **26** 3622 (1984) [*Sov. Phys. Solid State* **26** 2178 (1984)]
41. Rempel' A A, Gusev A I *Kristallografiya* **30** 1112 (1985) [*Sov. Phys. Crystallogr.* **30** 648 (1985)]
42. Gusev A I, Rempel A A *Phys. Stat. Sol. A* **93** (1) 71 (1986)
43. Bowman A L et al. *Acta Crystallogr.* **19** (Pt. 1) 6 (1965)
44. Lipatnikov V N et al. *Dokl. Akad. Nauk SSSR* **297** 849 (1987) [*Sov. Phys. Dokl.* **32** 988 (1987)]
45. Lipatnikov V N, Rempel' A A, Gusev A I *Zh. Neorg. Khim.* **33** 1860 (1988) [*Russ. J. Inorganic Chem.* **33** 1058 (1988)]
46. Gusev A I, Rempel A A, Lipatnikov V N *Phys. Stat. Sol. A* **106** (2) 459 (1988)
47. Rempel' A A, Lipatnikov V N, Gusev A I *Dokl. Akad. Nauk SSSR* **310** 878 (1990) [*Sov. Phys. Dokl.* **35** 103 (1990)]
48. Lipatnikov V N, Rempel A A, Gusev A I *Collected Abstr. of Intern. Conf.* "*Advanced Methods in X-ray and Neutron Structure Analysis of Materials*" (Praha, Czechoslovakia, 1990) p. 95
49. Gusev A I, Rempel' A A, Lipatnikov V N *Fiz. Tverd. Tela* (Leningrad) **33** 2298 (1991) [*Sov. Phys. Solid State* **33** 1295 (1991)]
50. Remeev A Sh, Karimov I A *Izv. Akad. Nauk Uzb. SSR Ser. Fiz.-Tekh. Mat. Nauk* **2** 87 (1986)
51. Kesri R, Hamar-Thibault S *Acta Met.* **36** (1) 149 (1988)
52. Rempel' A A *Effekty Uporyadocheniya v Nestekhiometricheskikh Soedineniyakh Vnedreniya* (Ordering Effects in Nonstoichiometric Interstitial Compounds) (Ekaterinburg:Nauka, 1992)
53. Khaenko B V, Sivak O P *Dokl. Akad. Nauk Ukr. SSR Ser. A* **1** 91 (1989)
54. Venables J D, Meyerhoff M H *Solid State Chem.: Proc. of 5th Mater. Res. Symp.* (NBS Special Publ. 364) (Berkeley, 1972) p. 583
55. Lipatnikov V N, Rempel' A A, Gusev A I *Zh. Fiz. Khim.* **62** 589 (1988) [*Russ. J. Phys. Chem.* **62** 285 (1988)]
56. Gusev A I *Philos. Mag. B* **60** (3) 307 (1989)
57. de Novion C H, Landesman J P *Pure and Appl. Chem.* **57** (10) 1391 (1985)
58. Kovalev O V *Neprivodimye Predstavleniya Prostranstvennykh Grupp* (Irreducible Representations of the Space Groups) (Kiev: Akad. Nauk Ukr. SSR, 1961)
59. Kovalev O V *Neprivodimye i Indutsirovannye Predstavleniya i Kopredstavleniya Fedorovskikh Grupp* (Irreducible and Induced Representations and Corepresentations of the Fedorov Groups) (Moscow: Nauka, 1986)
60. Landau L D *Zh. Eksp. Teor. Fiz.* **7** 19 (1937) [*Phys. Zs. Sowjet.* **11** 26 (1937)]
61. Landau L D, Lifshitz E M *Statistical Physics* (New York: Pergamon, 1984)
62. Khachaturyan A G *Teoriya Fazovykh Prevrashchenii i Struktura Tverdykh Rastvorov* (Theory of Phase Transformations and the Structure of Solid Solutions) (Moscow: Nauka, 1974)
63. Gusev A I, Rempel A A *J. Phys. C: Solid State Phys.* **20** (31) 5011 (1987)
64. Rempel' A A, Lipatnikov V N, Gusev A I *Kristallografiya* **32** 1032 (1987) [*Sov. Phys. Crystallogr.* **32** 607 (1987)]
65. Lipatnikov V N, Rempel' A A, Gusev A I *Fiz. Tverd. Tela* (Leningrad) **31** (10) 285 (1989) [*Sov. Phys. Solid State* **31** 1818 (1989)]
66. Gusev A I, Rempel' A A, Lipatnikov V N *Zh. Fiz. Khim.* **64** 2343 (1990) [*Russ. J. Phys. Chem.* **64** 1265 (1990)]
67. Athanassiadis T, Lorenzelli N, de Novion C H *Ann. Chim. Fr.* **12** (2) 129 (1987)
68. Williams W S *High Temp.-High Pressure* **4** (6) 627 (1972)
69. Rempel A A, Gusev A I *Phys. Stat. Sol. B* **130** (2) 413 (1985)
70. Rempel' A A , Gusev A I *Fiz. Met. Metalloved.* **60** 847 (1985) [*Phys. Met. Metallogr.* (GB) **60** 11 (1985)]
71. Rempel' A A, Gusev A I *Fiz. Tverd. Tela* (Leningrad) **32** 16 (1990) [*Sov. Phys. Solid State* **32** 8 (1990)]
72. Rempel A A, Gusev A I *Phys. Status Solidi B* **160** (2) 389 (1990)
73. Lipatnikov V N, Rempel' A A, Gusev A I *Khimiya Tverdogo Tela* (Solid State Chemistry) (Ed. A I Gusev) (Sverdlovsk: Ural'skiĭ Nauchnyi Tsentr 1989) p. 18
74. Lipatnikov V N, Rempel' A A, Gusev A I *Izv. Akad. Nauk SSSR, Neorg. Mater.* **26** 2522 (1990) [*Inorg. Mater. (USSR)* **26** 2171 (1990)]
75. Storms E K, Krikorian N H *J. Phys. Chem.* **63** (10) 1747 (1959)
76. Kempter C P, Storms E K, Fries R J *J. Chem. Phys.* **33** (6) 1873 (1960)
77. Santoro G *Trans. Met. Soc. AIME.* **227** (6) 1361 (1963)
78. Gusev A I *Phys. Stat. Sol. A* **111** (2) 443 (1989)
79. Rempel' A A, Gusev A I *Fiz. Tverd. Tela* (Leningrad) **27** 3678 (1985) [*Sov. Phys. Solid State* **27** 2216 (1985)]
80. Gusev A I, Rempel A A *Phys. Stat. Sol. B* **154** (2) 453 (1989)
81. de Novion C H, Maurice V *J. Phys. Collog.* **38** (7) C 211 (1977)
82. Moisy-Maurice V et al *Solid State Commun.* **39** (5) 661 (1981)
83. Metzger T H, Peisl J, Kaufmann R *J. Phys. F: Metal Phys.* **13** (6) 1103 (1983)
84. Schwarz K *CRC Critical Reviews in Solid State and Mater. Sci.* **13** (3) 211 (1987)
85. Gruzalski G R, Zehner D M *Phys. Rev. B* **34** (6) 3841 (1986)
86. Schadler G H et al. *Phys. Rev. B* **38** (14) 9538 (1988)
87. Cherkashenko V M, Rempel' A A, Gusev A I *Fiz. Tverd. Tela* (Leningrad) **27** 1387 (1985) [*Sov. Phys. Solid State* **27** (5) 838 (1985)]
88. Cherkashenko V M et al. *Zh. Neorg. Khimii* **36** 474 (1991) [*Russ. J. Inorganic Chem.* **36** 474 (1968)]
89. Rempel' A A, Gusev A I *Fiz. Tverd. Tela* (Leningrad) **25** 3169 (1983) [*Sov. Phys. Solid State* **25** 1827 (1983)]
90. Rempel A A, Gusev A I, Belyaev M Yu *J. Phys. C: Solid State Phys.* **20** (34) 5655 (1987)
91. Kurmaev E Z et al. *Zh. Strukt. Khim.* **22** 172 (1981)
92. Schwarz K, Rosch N *J. Phys.C: Solid State Phys.* **9** (16) L433 (1976)
93. Reis G, Winter H *J. Phys. F: Metal Phys.* **10** (1) 1 (1980)
94. Hochst H et al. *Ztschr. Phys. B* **37** (1) 27 (1980)
95. Gusev A I, Rempel A A *Phys. Stat. Sol. B* **151** (1) 211 (1989)

96. Men'shikov A Z, Kurmaev E Z *Fiz. Met. Metalloved.* **41** 748 (1976) [*Phys. Met. Metallogr.* (UK) **41** 748 (1976)]
97. Gusev A I, Rempel A A *Phys. Stat. Sol. A* **84** (2) 527 (1984)
98. Rempel' A A et al. *Izv. Akad. Nauk SSSR, Neorg. Mater.* **21** 596 (1985) [*Inorg. Mater.* (USSR) **21** 514 (1995)]
99. Blokhin M A, Shveitser I G *Rentgenospektral'nyi Spravochnik* (Handbook of X-ray Spectra) (Moscow: Nauka, 1982)
100. Rempel' A A, Sinel'nichenko A K *Metallofizika* **13** 61 (1991) [*Phys. Metals* **11** 352 (1992)]
101. Ramqvist L et al *J. Phys. and Chem. Solids.* **31** (12) 2669 (1970)
102. Ihara H, Hirabayashi M, Nakagawa H *Phys. Rev. B* **14** (4) 1707 (1976)
103. Ihara H, in *Res. of the Electrotechn. Lab.* № *775* (Tokyo: Electrotechnical Laboratory, 1977)
104. Zhukov V P et al. *Zh. Neorg. Khim.* **25** 318 (1980) [*Russ. J. Inorganic Chem.* **25** (1980)]
105. Landesman J P et al. *J. de Physique* **46** (6) 1001 (1985)
106. Blaha P et al. *J. Solid State Chem.* **70** (2) 199 (1987)
107. Nefedov V I *Rentgenoelektronnaya Spektroskopiya Khimicheskikh Soedinenii* (X-ray Spectroscopy of Chemical Compounds) (Moscow: Khimiya, 1984)
108. Maier K et al *Phys. Rev. Lett.* **39** (8) 484 (1977)
109. Maier K et al. *Philos. Mag. A* **40** 701 (1979)
110. Gupta R P, Siegel R W *J. Phys. F: Metal Phys.* **10** (1) L7 (1980)
111. Schaefer H-E, Forster M *Mater. Sci. Engineering A* **109** (2) 161 (1989)
112. Würschum R et al. *J. Phys.: Condens. Matter* **1** SA33 (1989)
113. Mikhalenkov V S *Metallofizika* **5** 44 (1983)
114. Rempel' A A et al. *Dokl. Akad. Nauk SSSR* **300** 92 (1988) [*Sov. Phys. Dokl.* **33** 367 (1988)]
115. Rempel' A A, Druzhkov A P, Gusev A I *Fiz. Met. Metalloved.* **68** 271 (1989) [*Phys. Met. Metallogr.* (UK) **68** 59 (1989)]
116. Rempel' A A, Druzhkov A P, Gusev A I *Fiz. Tverd. Tela* (Leningrad) **32** 1333 (1990) [*Sov. Phys. Solid State* **32** 779 (1990)]
117. Rempel' A A, Forster M, Schaefer H-E *Dokl. Akad. Nauk* (Russia) **326** 91 (1992) [*Phys. Dokl.* **39** 484 (1992)]
118. Rempel A A, Forster M, Schaefer H-E *J. Phys.: Condens. Matter* **5** (2) 261 (1993)
119. Rempel A A et al., in *Materials Research Soc. Symp. Proc. V. 327* (Pittsburgh, 1993) p. 299
120. Miron N F, Maev S N *Fiz. Met. Metalloved.* **66** 1159 (1988) [*Phys. Met. Metallogr.* (UK) **66** 1159 (1988)]
121. Novikov Yu A, Rakov A V, Shantarovich V P *Fiz. Tverd. Tela* (Leningrad) **36** 1710 (1994) [*Sov. Phys. Solid State* **36** 935 (1994)]
122. Dlubek G, Rechner W, Brummer O *Exper. Tech. Phys.* **25** (4) 289 (1977)
123. *Pozitronsoderzhashchie Sistemy i Pozitronnaya Diagnostika* (Positron-Containing Systems and Positron Diagnostics) (Ed. U A Arifov) (Tashkent: Fan, 1978)
124. Schaefer H E *Phys. Stat. Sol. A* **102** (1) 47 (1987)
125. Dekhtyar I Ya, Nemoshkalenko V V *Elektronnaya Struktura i Elektronnye Svoĭstva Perekhodnykh Metallov i Splavov* (Electronic Structure and Electronic Properties of Transition Metals and Alloys) (Kiev: Naukova Dumka, 1971)
126. Gol'danskiĭ V I *Fizicheskaya Khimiya Pozitrona i Pozitroniya* (Chemistry of the Positron and Positronium) (Moscow: Nauka, 1968)
127. Hudson D J *Statistics Lectures on Elementary Statistics and Probability* (Geneva, 1964)
128. Marksteiner P et al. *Phys. Rev. B* **33** (2) 812 (1986)
129. Marksteiner P et al. *Phys. Rev. B* **33** (10) 6709 (1986)
130. Trefilov V I et al. *Metallofizika* **10** (4) 18 (1988)
131. Seeger A, Banhart F *Phys. Stat. Sol. A* **102** (1) 171 (1987)
132. Puska M J et al. *Phys. Rev. B* **49** 10947 (1994)
133. Gosset D et al. *Radiation Effects and Defects in Solids* **118** (2) 207 (1991)
134. Allison C Y, Stoller R E, Kenik E A *J. Appl. Phys.* **63** (5) 1740 (1988)
135. Das G, Chatterjee D K, Lipsitt H A *J. Mater. Sci.* **16** (12) 3283 (1981)
136. Lorenzelli N et al. *Solid State Commun.* **59** (11) 765 (1986)
137. Shacklette L W, Williams W S *Phys. Rev. B Solid State* **7** (12) 5041 (1973)
138. Emmons G H, Williams W S *J. Mater. Sci.* **18** 2589 (1983)
139. Dy, L C Williams W S *J. Appl. Phys.* **53** 8915 (1982)
140. Gusev A I, Rempel' A A *Fiz. Tverd. Tela* (Leningrad) **27** 1528 (1985) [*Sov. Phys. Solid State* **27** 920 (1985)]
141. Rempel' A A et al. *Fiz. Tverd. Tela* (Leningrad) **28** 279 (1986) [*Sov. Phys. Solid State* **28** 153 (1986)]
142. Dubrovskaya L B, Nazarova S Z, Kachkovskaya E T *Izv. Akad. Nauk SSSR, Neorg. Mater.* **20** 783 (1985) [*Inorg. Mater.* **20** (5) 674 (1985)]
143. Toth L E *Transition-Metal Carbides and Nitrides* (New York: Academic Press, 1971)
144. Vonsovskiĭ S V, Izyumov Yu A, Kurmaev E Z *Sverkhprovodimoct' Perekhodnykh Metallov, ikh Splavov i Soedineniĭ* (Superconductivity of the Transition Metals and of their Alloys and Compounds) (Moscow: Nauka, 1977)
145. Giorgi A L et al. *Phys. Rev.* **125** (3) 837 (1962)
146. Willens R H, Buehler E, Matthias B T *Phys. Rev.* **159** (2) 327 (1967)
147. Toth L E, Ishikawa M, Chang Y A *Acta Met.* **16** (9) 1183 (1968)
148. Dubrovskaya L B, Rabin'kin A G, Gel'd P V *Zh. Eksp. Teor. Fiz.* **62** 300 (1972) [*Sov. Phys. JETP* **35** 161 (1972)]
149. Rempel' A A et al. *Zh. Fiz. Khim.* **61** 1761 (1987) [*Russ. J. Phys. Chem.* **61** 919 (1987)]
150. Shacklette L W, Radosevich L G, Williams W S *Phys. Rev. B. Solid State* **4** (1) 84 (1971)
151. McMillan W L *Phys. Rev.* **167** (2) 331 (1968)
152. Borukhovich A S et al. *Phys. Stat. Sol. B* **45** (1) 179 (1971)
153. Morinaga M et al. *Philos. Mag. B* **47** (1) 107 (1983)
154. Rempel' A A, Gusev A I *Tez. Konf. 'Metallofizika Sverkhprovodnikov'* ('Physics of Superconducting Metals' (Abstracts)) (Kiev: Institut Akad. Nauk Ukr. SSR, 1986) p. 1. p. 76.
155. Khlyustikov I N, Moskvin S I *Zh. Eksp. Teor. Fiz.* **89** 1846 (1985) [*Sov. Phys. JETP* **62** 1065 (1985)]
156. Buzdin A I, Khvorikov N A *Zh. Eksp. Teor. Fiz.* **89** 1857 (1985) [*Sov. Phys. JETP* **62** 1071 (1985)]
157. Karimov Yu S, Utkina T G *Pis'ma Zh. Eksp. Teor. Fiz.* **51** 468 (1990) [*JETP Letters* **51** 468 (1990)]
158. Rempel' A A, Gusev A I *Zh. Fiz. Khim.* **62** 2897 (1988) [*Russ. J. Phys. Chem.* **62** 1509 (1988)]
159. Rempel A A, Gusev A I *Phys. Stat. Sol. A* **113** (2) 353 (1989)
160. Leibfried G *Gittertheorie der Mechanischen und Thermischen Eigenschaften der Kristalle* (Berlin: Springer-Verl., 1955)
161. de Novion C H, Landesman J P *Pure and Appl. Chem.* **57** (10) 1391 (1985)